



AD

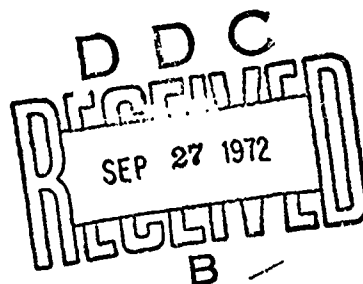
RESEARCH AND DEVELOPMENT
TECHNICAL REPORT ECOM-0129-F

1975
888
888
888
888
AD
AD

A
**THEORETICAL AND EXPERIMENTAL
INVESTIGATION OF PLANAR
PIN THERMOPHOTOVOLTAIC
CELLS**

FINAL REPORT

By
R. J. Schwartz
N. F. Gardner



AUGUST 1972

SEE AD 23071

ECOM

UNITED STATES ARMY ELECTRONICS COMMAND • FORT MONMOUTH, N.J.

CONTRACT DAAB07-70-C-0129

SCHOOL OF ELECTRICAL ENGINEERING
PURDUE UNIVERSITY
WEST LAFAYETTE, INDIANA

DISTRIBUTION STATEMENT
Approved for public release;
distribution unlimited

Reproduced by
NATIONAL TECHNICAL
INFORMATION SERVICE
U S Department of Commerce
Springfield VA 22151

**Best
Available
Copy**

NOTICES

Disclaimers

The findings in this report are not to be construed as an official Department of the Army position, unless so designated by other authorized documents.

The citation of trade names and names of manufacturers in this report is not to be construed as official Government indorsement or approval of commercial products or services referenced herein.

Disposition

Destroy this report when it is no longer needed. Do not return it to the originator.

ACCESSION FOR	
NTIS	White Section <input checked="" type="checkbox"/>
BGS	Buff Section <input type="checkbox"/>
UNARMEDIZED	<input type="checkbox"/>
JUSTIFICATION	
.....	
BY	
DISTRIBUTION/AVAILABILITY CODES	
DIST.	A/AIL. AND/OR SPECIAL
A	

Security Classification

DOCUMENT CONTROL DATA - R & D

(Security classification of title, body of abstract and indexing annotation must be entered when the overall report is classified)

1. ORIGINATING ACTIVITY (Corporate author) Purdue University Lafayette, Indiana 47907	2a. REPORT SECURITY CLASSIFICATION Unclassified
	2b. GROUP

3. REPORT TITLE

A Theoretical and Experimental Investigation of Planar PIN Thermophotovoltaic Cells

4. DESCRIPTIVE NOTES (Type of report and Inclusive dates)

Final Report (June 1970 - June 1972)

5. AUTHOR(S) (First name, middle initial, last name)

R. J. Schwartz and N. F. Gardner

6. REPORT DATE August 1972	7a. TOTAL NO. OF PAGES 85	7b. NO. OF REFS
8a. CONTRACT OR GRANT NO. DAAP07-70-C-0129	9a. ORIGINATOR'S REPORT NUMBER(S)	
b. PROJECT NO. 1TO 61102 A 30 A		
c. Task No. -02	9b. OTHER REPORT NO(S) (Any other numbers that may be assigned this report) ECOM-0129-2	
d. Subtask No. -312		

10. DISTRIBUTION STATEMENT

Approved for public release; distribution unlimited.

11. SUPPLEMENTARY NOTES	12. SPONSORING MILITARY ACTIVITY US Army Electronics Command ATTN: AMSEL-TL-RB Fort Monmouth, New Jersey 07703
-------------------------	---

13. ABSTRACT

The results of calculations of the performance of a planar p-i-n thermophotovoltaic cell are reported. A computer program has been written which automatically optimizes the cell geometry. The program allows the bulk recombination rate, the surface recombination velocity, the hole and electron mobilities and the intensity and spectrum of radiation illuminating the cell to be chosen arbitrarily. The performance of germanium p-i-n cells is investigated for monochromatic radiation and radiation from 1873°K erbium oxide and black body sources.

Experimental work leading to the fabrication of interdigitated p-i-n thermophotovoltaic cells is described. The results of tests evaluating the performance of fabricated cells are discussed. A series of experiments were carried out to determine why the performance of these cells was below theoretical expectations.

Details of illustrations in
this document may be better
studied on microfiche

DD FORM 1473 1 NOV 68

REPLACES DD FORM 1473, 1 JAN 64, WHICH IS
OBSOLETE FOR ARMY USE

Security Classification

Security Classification

4 KEY WORDS	LINK A		LINK B		LINK C	
	ROLE	WT	ROLE	WT	ROLE	WT
Thermophotovoltaic Energy Conversion Photovoltaic Cell Germanium PIN-Junction Device						

TR ECOM-0129-F
AUGUST 1972

REPORTS CONTROL SYMBOL
OSD - 1366

A THEORETICAL AND EXPERIMENTAL
INVESTIGATION OF PLANAR PIN
THERMOPHOTOVOLTAIC CELLS

REPORT NO. 2
JUNE 1970-JUNE 1972
CONTRACT NO. DAABO7-70-C-0129
DA PROJECT NO. ITO 61102 A36A-02-31

Prepared By
R. J. Schwartz
N. F. Gardner
School of Electrical Engineering
PURDUE UNIVERSITY
West Lafayette, Ind.

For
U.S. Army Electronics Command
Fort Monmouth, N. J.

Distribution Statement
Approved for public release;
distribution unlimited

ABSTRACT

The results of calculations of the performance of a planar p-i-n thermophotovoltaic cell are reported. A computer program has been written which automatically optimizes the cell geometry. The program allows the bulk recombination rate, the surface recombination velocity, the hole and electron mobilities and the intensity and spectrum of radiation illuminating the cell to be chosen arbitrarily. The performance of germanium p-i-n cells is investigated for monochromatic radiation and radiation from 1873°K erbium oxide and black body sources.

Experimental work leading to the fabrication of interdigitated p-i-n thermophotovoltaic cells is described. The results of tests evaluating the performance of fabricated cells are discussed. A series of experiments were carried out to determine why the performance of these cells was below theoretical expectations.

CONTENTS

	<u>Page</u>
LIST OF SYMBOLS	-iv-
LIST OF TABLES	-v-
LIST OF FIGURES	-vi-
INTRODUCTION	1
I. THEORETICAL INVESTIGATIONS	4
A. Introduction	4
B. Lifetime Considerations	4
C. Results	6
1. Monochromatic radiation	6
2. Radiation from an erbium oxide source	15
3. Radiation from a black body Source	22
II. EXPERIMENTAL INVESTIGATIONS	24
A. Introduction	24
B. Description of Device Fabrication Process	24
C. Experimental Investigations of the Fabrication Process	26
1. Insulator deposition	26
Silicon dioxide deposition	26
Aluminum oxide deposition	27
Photoresist problems with silicon dioxide films	27
2. Contact formation	27
n contacts	28
Chemical etching	30
Ultrasonic etching	30
Photoresist liftoff etching	30
Arsenic doped contacts	31
p contacts	31
Alloying	32
Junction staining solution	32
Alloying technique	33
Aluminum films	33
Indium films	34
Aluminum on indium films	34
Antimony on gold films	34
Antimony films	35
Tin-Antimony-tin films	35
Conclusions	35
Contact buildup	36

	<u>Page</u>
3. Fabrication problems	37
Compatibility of etchants and processing chemicals	37
Problems with gold contacting aluminum	37
4. Heat sink fabrication and device mounting	40
5. Evaluation of heat sink performance	41
D. Performance of Fabricated Devices	42
E. Investigation of Deficiencies in Devices	45
1. Contact Deficiencies	45
2. Lifetime damage due to silicon dioxide deposition	46
3. Determination of the dominant source of recombination	49
4. Conclusions	53
III. CONCLUSIONS AND RECOMMENDATIONS FOR FUTURE WORK	54
REFERENCES	56
APPENDIX	57
PRINTOUT OF ADOP PROGRAM	72

SYMBOL LIST*

l_n = width of n contact

l_p = width of p contact

l_i = spacing between contacts

x_0 = thickness of device

n = excess carrier concentration

e = electron charge

n_i = intrinsic carrier concentration

V = voltage

k = Boltzmann's constant

T = temperature in °K

* All symbols used in the FORTRAN program are defined in Tables XII and XIII.

TABLES

	<u>Page</u>
I. Optimum Dimensions and Output Parameters of Devices Illuminated with Monochromatic Radiation	8
II. Dependence of Output Parameters on Device Thickness	10
III. Variation in Maximum Power Output for Different Contact Widths	13
IV. Optimum Dimensions and Output Parameters of Devices Illuminated with 1873°K Erbium Oxide Spectrum	16
V. Optimum Dimensions and Output Parameters of Devices with Finite Bulk Lifetimes	20
VI. Optimum Dimensions and Output Parameters of Devices Illuminated with 1873°K Black Body Spectrum	23
VII. Effects of Chemicals and Etchants on Metals and Insulators	38
VIII. Etchants Used in Device Fabrication	39
IX. Open Circuit Voltage Output of Fabricated Devices	43
X. Open Circuit Voltage Output of Dot Pattern Devices	47
XI. Effect of Silicon Dioxide Deposition on Excess Carrier Concentration	51
XII. Relative Conductivity as a Function of Surface Bias	52
XIII. List of Physical Parameters	61
XIV. List of Output Parameters	64
XV. Printed Output for a Given Set of Dimensions	67
XVI. Summary of Outputs for Given Sets of Dimensions and Output for Optimized Device	68

FIGURE LIST

	<u>Page</u>
FIGURE 1 Planar p-i-n Thermophotovoltaic Cell	2
FIGURE 2 Excess Carrier Concentration and Open Circuit Voltage at Which Bulk Radiative Recombination Equals Bulk Trap Recombination	5
FIGURE 3 Performance Characteristics for Cells Optimized for Monochromatic Radiation	11
FIGURE 4 Current - Voltage Curves of Devices Illuminated with Erbium Oxide Spectrum	17
FIGURE 5 Performance Characteristics of Cell Optimized for Radiation from an Erbium Oxide Source	19
FIGURE 6 Current - Voltage Curves of Devices with Finite Bulk Lifetimes	21
FIGURE 7 Partially Fabricated p-i-n Thermophotovoltaic Cell	25
FIGURE 8 Completely Fabricated p-i-n Thermophotovoltaic Cell	25
FIGURE 9 p-i-n Cell Mounted in Water Cooled Heat Sink	41
FIGURE 10 Current-Voltage Curve for Device #6	44
FIGURE 11 Current-Voltage Curve for Device #6 with Reverse Bias Applied	44
FIGURE 12 Sample Used to Test Effect of Silicon Dioxide Deposition on Lifetime.	48
FIGURE 13 Apparatus Used to Test Effect of Silicon Dioxide Deposition on Lifetime	50

INTRODUCTION

This is a final report on the work which was performed under contract number DAAB07-70-C-0129. This report contains a detailed description of the work performed from June 1, 1971 to June 1, 1972 under the above contract. Previous work covering the period from June 1, 1970 to June 1, 1971 which was performed under the same contract has been reported in the annual report TR ECOM-OI29-1. This report, which will be referred to as Report No. 1,¹ was published in August, 1971 with the control symbol OSD-1366.

The purposes of this contract were to theoretically investigate germanium p-i-n planar photovoltaic cells, to determine the optimum design of such cells for thermophotovoltaic use and to fabricate germanium p-i-n cells which represent the present state of the art. Figure 1 shows a cross section view and a view from the contact side of a planar p-i-n structure.

One of the purposes of this investigation is to determine if the p-i-n structure has a significant advantage over the standard p-n photovoltaic cell in thermophotovoltaic applications. In order to do this, the performance of the p-i-n cell had to be analyzed under a variety of operating conditions. This was done with a computer program which would allow the computation of cell performance under a variety of specified incident radiation spectra as well as a variety of materials parameters such as surface recombination velocity, bulk recombination rate and mobility. The computer program was described in Report No. 1.¹ During the last year of the contract this program has been expanded to allow for automatic optimization of the device dimensions when the incident radiation spectrum,

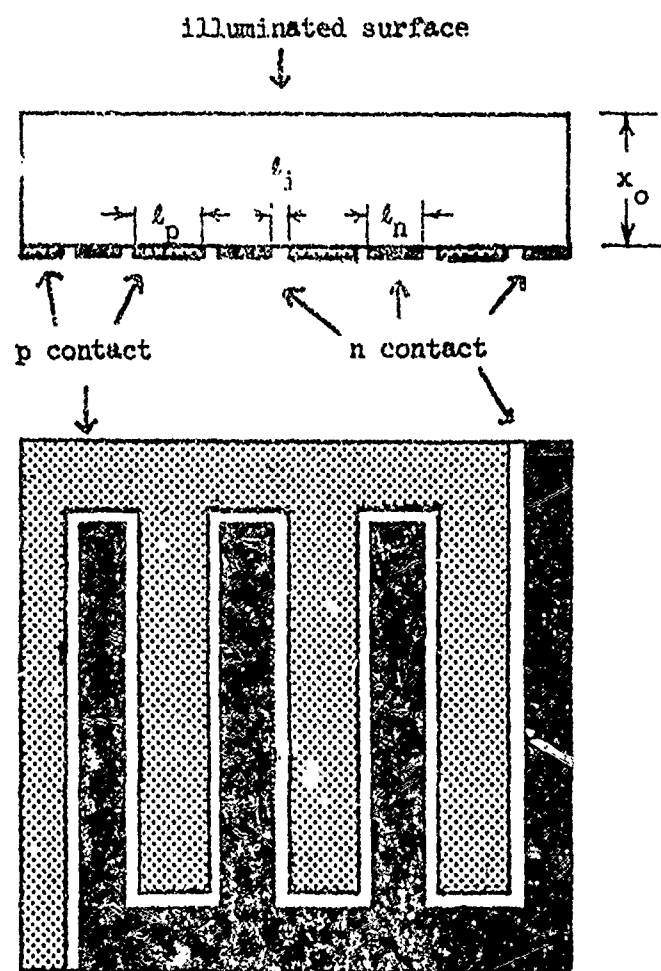


Figure 1. Planar p-i-n Thermophotovoltaic Cell

surface recombination velocity and the bulk recombination rate are specified. The first part of this report deals with the results of this optimization program.

Three distinct types of radiation spectra were selected for study - monochromatic radiation, black body radiation at 1873°K and radiation from an erbium oxide radiator at 1873°K. The analysis with monochromatic radiation is of little practical value, but it provides insight into the performance of the cell with other radiation spectra. The analysis with the erbium oxide radiator is of interest, because the spectral emissivity of erbium oxide is relatively large for photons with energies near the direct gap in germanium and relatively small for photons with energies well above or well below the direct gap energy. Thus, radiation from an erbium oxide source can be converted into electrical energy more efficiently than radiation from a black body source.

The second part of this report deals with the experimental program. It contains a description of the procedure used to fabricate p-i-n photovoltaic cells and of the investigations that were carried out in connection with the fabrication process. The results which have been obtained to date on the performance of germanium p-i-n photovoltaic cells are discussed. A series of tests was carried out to determine why the performance of these cells is below theoretical expectations.

In the third part of the report the most significant theoretical and experimental results are briefly discussed and recommendations are made for future work.

I. THEORETICAL INVESTIGATIONS

A. Introduction

In Report No. 1¹ the results of the program to optimize the design for a device illuminated by black body radiation were described. It was clear from these results that additional optimization calculations needed to be performed to determine the effects of various spectra as well as the effects of changes in surface recombination velocity and bulk recombination rate on the performance of the device. A new program was written which utilized essentially the same approach for evaluating the performance of the device as the program described in Report No. 1¹ but which also automatically optimized the dimensions of the device. This Automatic Device Optimization Program (ADOP) is described in the appendix.

B. Lifetime Considerations

In Report No. 1 we pointed out that in the usual operating range for a p-i-n photovoltaic cell, the lifetime of the excess carriers will be determined primarily by radiative recombination rather than by recombination through trap sites. In Figure 2 we show a curve of the excess carrier concentration as a function of minority carrier lifetime for which the rate of recombination due to recombination through trap sites is equal to the rate of recombination due to radiative recombination. The curve is also plotted in terms of open circuit voltage which can be correlated directly to excess carrier concentration. If the open circuit voltage for a particular minority carrier lifetime lies above the curve, the dominant recombination mechanism will be radiative

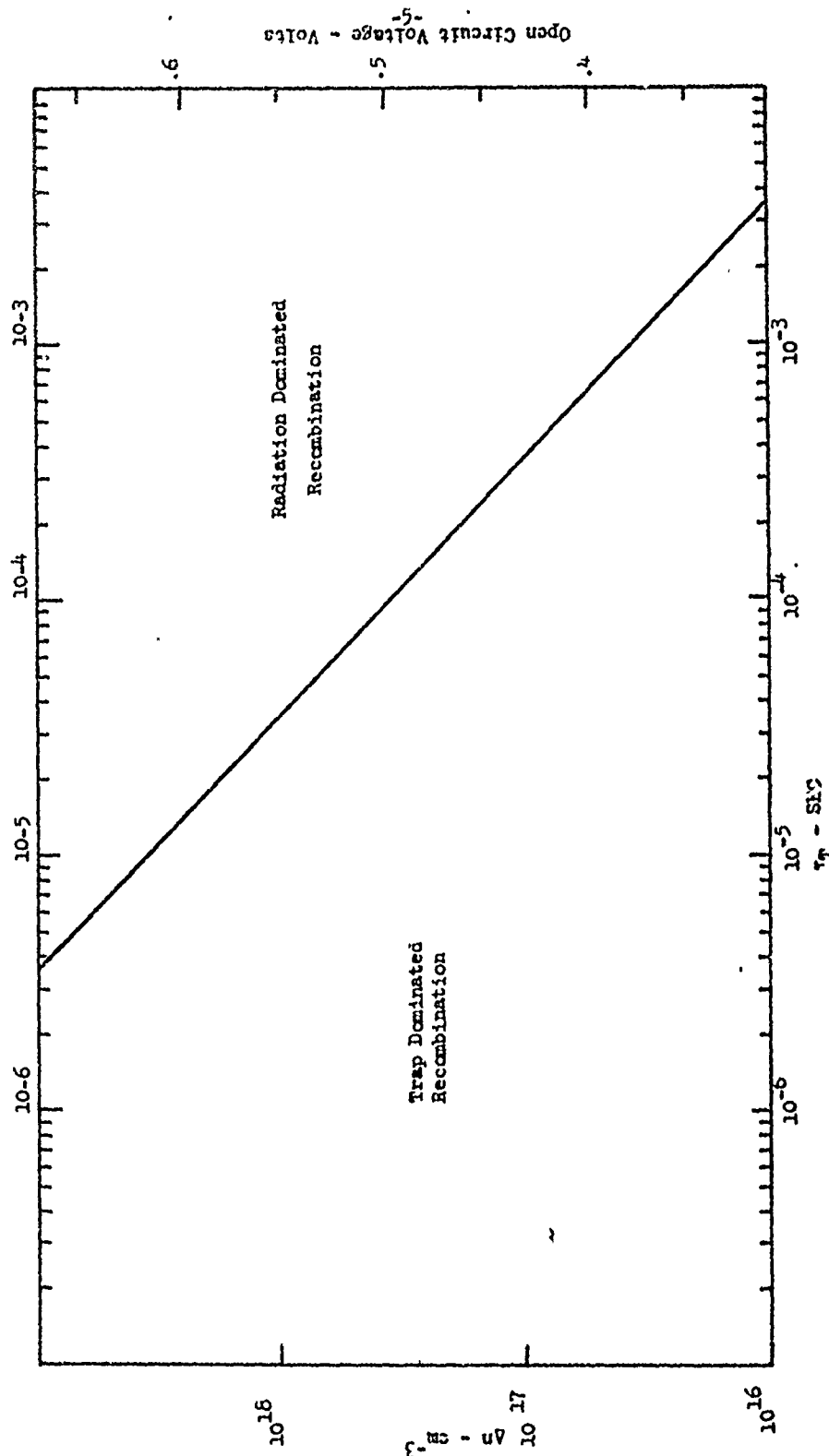


Figure 2. Excess Carrier Concentration and Open Circuit Voltage at Which Bulk Radiative Recombination Equals Bulk Trap Recombination

recombination. If the open circuit voltage lies below the curve, the dominant recombination mechanism will be recombination through trap sites. Since the minority carrier lifetime for the starting material is in excess of 2×10^{-3} seconds, it appears that for operating conditions which would normally be found in the operation of a photovoltaic cell, ($\Delta N 10^{17}$ electrons cm^{-3}) the dominant recombination mechanism would be radiative recombination. If, however, the minority carrier lifetime in the bulk is significantly reduced during processing (say to a value of 10 to 100 μ sec.), then the dominant recombination mechanism would not be radiative recombination, and one should base lifetime calculations on the usual Hall-Shockley-Reed type recombination statistics. Since the purpose of using intrinsic material is to obtain a very high minority carrier lifetime in the bulk, we have assumed for all of our calculations that the dominant recombination mechanism is radiative recombination. The radiative recombination parameter is found to be equal to 2.8×10^{-17} $\text{cm}^3 \text{sec}^{-1}$ from fundamental thermodynamic arguments.⁶ None of the devices, which are described in chapter II, were operated in the radiation recombination region during performance tests, performed under this contract. The reasons for this are discussed in chapters II and III.

C. Results

The results obtained from the ADOL program are summarized in Tables I, II, V and VI. The results for monochromatic radiation will be analyzed in considerable detail. Many of the conclusions drawn from these results will be applicable to those obtained for black body radiation and radiation from an erbium oxide source.

1. Monochromatic radiation

The performance of the n-i-n cell has been analyzed for three different wavelengths of monochromatic radiation. The wavelengths were chosen so that their absorption lengths would vary over a range of values which would be

approximately equal to realistic values of device thickness (x_0). The three wavelengths chosen were $1.50 \mu\text{m}$, $1.54 \mu\text{m}$ and $1.60 \mu\text{m}$ with respective absorption lengths of $2.3 \mu\text{m}$, $21 \mu\text{m}$ and $104 \mu\text{m}$. An absorbtion length is defined as the distance into the germanium at which 63% of the incident radiation has been absorbed.

The results of the output obtained from the ADOP program for monochromatic radiation are summarized in Table I, and Figure 3. The spacing between contacts (LI) is fixed at $25 \mu\text{m}$. The maximum current collectable per unit area of illuminated surface, if every photon capable of generating a hole-electron is absorbed (CBHDOPT), is fixed at 5 amps/cm^2 . The following observations can be made from the results in Table I:

1) When the excess carrier concentration is very large, the optimum device thickness is determined primarily by two conflicting factors. The device should be as thick as possible in order to absorb as much of the incident radiation as possible. On the other hand, as the device gets thicker the volume in which recombination can take place increases, while the relative increase in the number of photons absorbed tends to become smaller. Therefore the excess carrier concentration must decrease. This, of course, results in a reduction of output voltage.

The dependence of open circuit voltage and short circuit current on device thickness is shown in Table II. The data in this Table is obtained from the output of the program from which device 11 was optimized. Note that as X_0 increases, the open circuit voltage and maximum power point voltages decrease, while the short circuit current and maximum power point current increase.

In cases where VSB and VST are both 0 (devices #1, 11 and 20), the optimum thickness (X_0) is roughly four absorption lengths. About 90% of the incident photons are absorbed in four absorption lengths.

TABLE I
Optimum Dimensions and Output Parameters of Devices Illuminated With Monochromatic Radiation*

Device	Absorpti ^{on}	Wavelength	Absorpti ^{on}	Wavelength	RCOPFC = $2.8 \times 10^{-4} \text{ cm}^3 \text{ sec.}^{-1}$	CURRSC (amp cm ⁻²)	VOC (Volts)	
							MAXPOW (W)	MAXPOW (Watt)
1	0	12.18	20.29	22.98	2.224	67.80	1.000	.9938
2	0	30.62	50.56	50+	2.049	62.10	1.000	.9938
3	10	116.7	200.9	50+	1.963	59.47	.999	1.000
4	100	130.5	224.4	50+	1.594	46.29	.9893	1.000
5	1000	169.26	146.1	50+	.9551	28.94	.9036	1.000
6	0	10	30.67	51.14	50+	1.976	.991	.9991
7	0	100	30.76	51.74	50+	1.634	49.50	.9909
8	0	1000	31.34	55.25	50+	1.027	31.13	.9164
9	10	0	132.9	224.7	50+	2.034	61.65	.9929
10	100	0	332.5	523.0	50+	1.986	60.17	Unreliable
11	0	0	56.25	83.57	91.63	1.942	.991	.9999
12	10	10	123.0	203.7	99.33	1.879	.9745	.9964
13	100	100	169.0	282.3	114.5	1.570	.4779	.9910
14	1000	1000	136.4	210.4	94.63	.9569	29.29	.9941
15	0	10	56.19	83.72	98.47	1.886	.9776	.9986
16	0	100	56.27	64.36	111.6	1.601	.4672	.9946
17	0	1000	56.82	87.56	84.65	.9959	30.64	.9946
18	10	0	132.3	219.2	93.05	1.931	.9926	.9999
19	100	0	321.1	522.0	97.43	1.896	.58.03	Unreliable

(Continued on next page)

(Table I continued)

Device	Absorpti on	Length = 2.00 m	Wave Length = 1.06 μ m	Intensity	VSB (cm sec ⁻¹)	VST (cm sec ⁻¹)	MAXPOW (Watt cm ⁻²)	ETACOL (%)	ETABBS	E (Volts)	CURRSC (amp cm ⁻²)
20	0	128.1	197.2	376.0	1.694	52.81	.9969	.9722	.7658	.4565	4.846
21	.10	154.6	236.9	381.7	1.661	51.69	.9922	.9738	.7563	.4546	4.831
22	.100	215.7	350.4	390.6	1.437	44.59	.9534	.9762	.7044	.4407	4.654
23	.1000	216.1	360.5	297.0	.7865	25.30	.7754	.9420	.5868	.3670	3.652
24	0	10	119.7	187.0	380.6	1.664	51.60	.9923	.9736	.7575	.4584
25	0	100	126.6	197.0	383.7	1.452	45.01	.9533	.9756	.7064	.4420
26	0	1000	146.0	226.6	297.7	.6139	26.17	.7742	.9424	.6000	.3718
27	.10	0	156.3	236.9	371.2	1.691	52.69	.9968	.9724	.7646	.4563
26	.100	0	276.8	460.9	360.9	1.672	52.06	.9964	.9736	.7574	.4533
											4.650

* The FORTRAN variables given in this table are defined on pages in Table XIV. The estimated error in values of MAXPOW is 1% or less. The values in the Table are listed as they appeared in the computer program printout. Although the output values are generally inaccurate beyond the second decimal place, small differences between two corresponding output values for different values of input parameters will generally be accurate to the third or fourth decimal place.

[†] Devices #1 through #10 are optimized under the constraint that the minimum attainable device thickness is 50 μ m, because of limitations in fabrication technology.

TABLE II

Dependence of Output Parameters on Device Thickness*

$$\lambda = 1.54 \mu\text{m}$$
$$LN = 50 \mu\text{m} \quad LP = 75 \mu\text{m} \quad V_{SB} = V_{ST} = 0$$

XO (μm)	VOC (volts)	CURDESC (amp cm^{-2})	VMAXPOW (volts)	CMAXPOW (amp cm^{-2})	PMAXPOW (watt cm^{-2})
25.0	.5186	3.475	.4441	3.274	1.454
37.5	.5127	4.158	.4385	3.913	1.716
50.0	.5075	4.535	.4334	4.263	1.848
62.5	.5029	4.743	.4289	4.455	1.911
75.0	.4988	4.858	.4249	4.558	1.937
87.5	.4951	4.921	.4213	4.614	1.944
100	.4918	4.956	.4181	4.642	1.941
125	.4861	4.986	.4124	4.661	1.922
150	.4814	4.995	.4077	4.661	1.900
175	.4773	4.997	.4035	4.656	1.879
200	.4738	4.996	.3999	4.648	1.859

* The FORTRAN variables given in this table are defined in Table XIV. The data is obtained from the output of the program from which device 11 of Table I was optimized.

Performance Characteristics for cell optimized for
Non-chromatic radiation. See Table I. CDRDSC=5.0 amps.

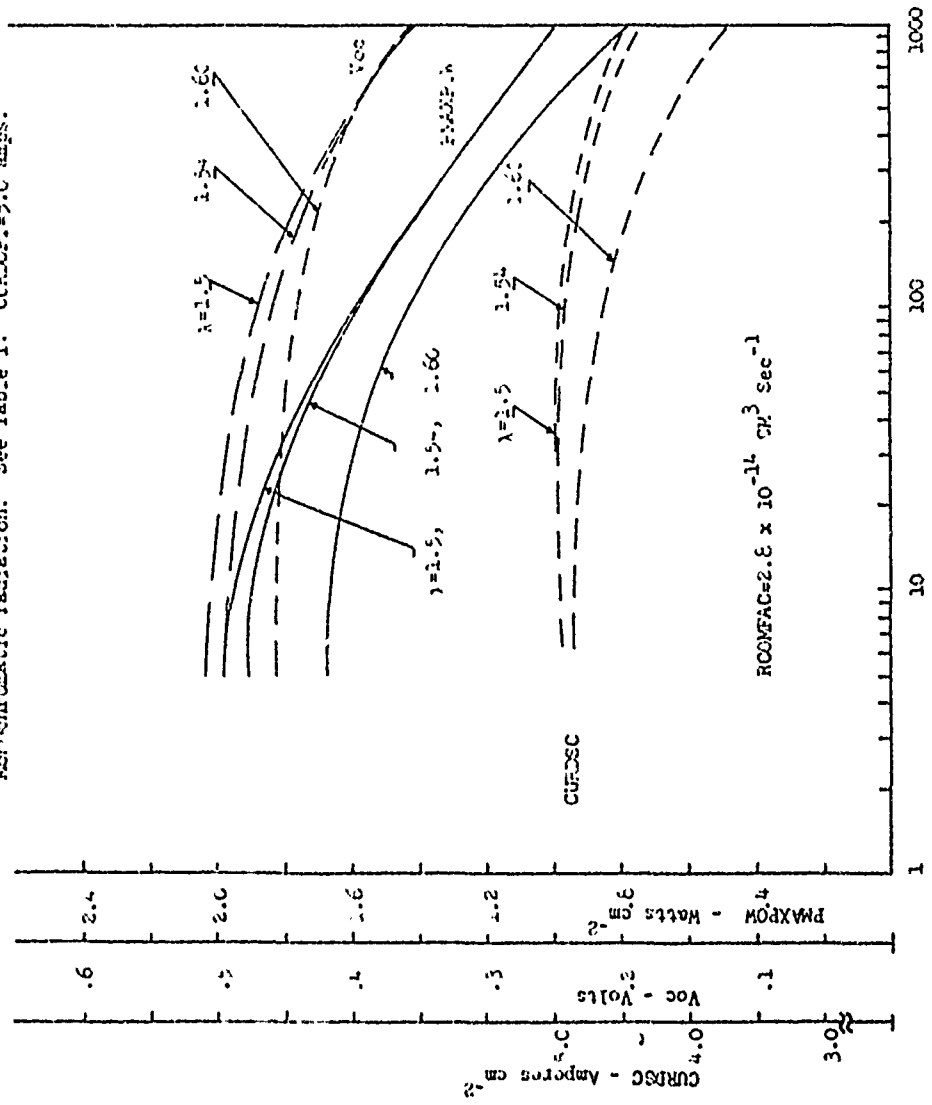


Figure 3. SURFACE REIONIZATION VELOCITY - cm sec^{-1}

2) In cases where VST and VSB are both 0 (device #1, 11 and 20), PMAXPOW increases as the absorption length decreases. This is because the optimum value of X_0 is smaller and therefore the volume in which excess carriers are generated is smaller. Hence, the number of carriers generated per unit volume is greater, and the open circuit voltage developed at the contacts is greater. This conclusion can be collaborated by a comparison of open circuit voltages for devices 1, 11 and 20. Note that the relative variation in open circuit voltage is much greater than the relative variation in short circuit current.

A second advantage resulting from larger excess carrier concentrations is a reduction in the resistivity of the bulk and, therefore, a reduction in ohmic loss due to the flow of current between contacts. However, this effect is almost negligible for the large excess carrier concentrations in devices 1, 11 and 20.

3) It would appear that the optimum contact widths LN and LP exhibit a strong dependence on the surface recombination velocity. For instance, in the case of devices 2 and 3, a small increase in the values of VSB and VST from 0 to 10 cm sec⁻¹ causes the optimum value of LN to change from 31 μm to 119 μm and the optimum value of LP to change from 51 μm to 201 μm . These changes, however, are not significant; for even though the optimum contact sizes change greatly, the output power is quite independent of contact sizes for small values of surface recombination velocity. This is shown for devices 2 and 3 in Table III. These devices are illuminated with radiation of a 1.50 μm wavelength. The output power shows similar lack of dependence on LN and LP for samples illuminated with radiation of other wavelengths when surface recombination velocities are small.

TABLE III

Variation in Maximum Power Output for Different Contact Widths
(Devices 2 and 3 from Table I)

$$X_0 = 50 \mu\text{m}$$

VBS (cm sec ⁻¹)	VST (cm sec ⁻¹)	LN (μm)	LP (μm)	PMAXPOW (watt cm ⁻²)
0	0	30.6*	51.0*	2.049
		5	100	2.048
		25	100	2.048
		12.5	50	2.048
		25	37.5	2.049
10	10	118.7*	200.9*	1.963
		150	250	1.962
		50	250	1.960
		50	200	1.961
		150	150	1.962

*Optimized dimensions.

4) As VSB increases while VST is held constant at 0 (devices 9, 10, 18, 19, 27 and 28), there is a tendency for LN and LP to increase. The effect of increasing LN and LP while holding LI constant is to decrease the fraction of the unilluminated surface which is subject to surface recombination. Thus, fewer excess carriers are lost due to recombination on the unilluminated surface. This tendency for the contact size to increase is counterbalanced by an increase in the series resistance in the device as the average distance between the center of the p contact and the center of the n contact is increased. Thus, as the recombination velocity on the rear surface increases from a value of zero to a larger value, we observe LN and LP increasing until the series resistance begins to dominate.

5) In cases where VST is increases while VSB is held at 0 (devices 15-17 and 24-26) there is a tendency for the device thickness to increase slightly until VST exceeds 100 cm/sec. The tendency for the optimum device thickness to increase can be accounted for by realizing that as the surface recombination velocity increases the relative importance of bulk recombination velocity decreases. As X_0 increases, the average excess carrier density decreases. This in turn, decreases the total recombination. Increasing X_0 also increases the number of carriers generated, although the effect is quite small when X_0 is greater than three absorption lengths. As the excess carrier concentration decreases, VOC decreases. Thus, the optimum value of X_0 represents the best compromise between these competing needs. The optimum value of X_0 will change as the relative importance of the surface recombination changes.

When the surface recombination velocity exceeds 100 cm sec^{-1} , the optimum thickness tends to decrease. This is because the excess carrier concentration becomes low enough to invalidate the assumption that the

excess carrier distribution is fairly uniform in the bulk region. Since most of the excess carriers are generated within one absorption length of the illuminated surface and since these carriers must diffuse to the contacts to be collected, the excess carrier concentration in the region of the contacts tends to be significantly less than the average excess carrier concentration in the bulk region when there is an appreciable current flowing through the contacts. Thus the maximum power point voltage will tend to be significantly reduced. The device tends to become thinner to minimize the reduction of excess carrier concentration in the region of the contacts due to the diffusion gradient.

6) In cases where VST and VSB are held equal (devices 2-5, 11-14 and 20-23), the effects of surface recombination occurring on the illuminated surface only and on the unilluminated surface only are combined. Thus, IN and LP increase as VSB increases to 100 cm sec.^{-1} , and (for devices 11-14 and 20-23) XO increases as VST increases to 100, but starts to decrease as VST increases to 1000.

2. Radiation from an erbium oxide source

The results obtained from the ADOP program for devices illuminated with radiation from an 1873°K erbium oxide source are summarized in Tables IV and V. The current-voltage curves of these devices are plotted Figures 4 and 6. In general the observations made for devices illuminated with monochromatic radiation are applicable to these devices.

For an idealized device (device 29) the conversion efficiency is 14.7%. If VST is held at 0, very little degradation of output power occurs for values of VSB smaller than 100 cm sec.^{-1} . On the other hand, if VSB is held at 0, there is a significant degradation in the output power

TABLE IV
Optimum Dimensions and Output Parameters of Devices Illustrated with 1873°K Erbium Oxide Spectrum*

DEVICE #	VSD sec. ⁻¹	L1 = 25 μm	ROOFAC = 2.8 × 10 ⁻¹⁴ cm ³ /sec	MAX				MIN				EVAL	SAB	E	G	GRADS (VOLTS)
				E	G	B	MAX	E	G	B	MAX					
Incident Power = 9.2 watt cm ⁻²	29	0	128.5	196.8	401.2	1.350	51.79	.9966	.7894	.7634	.4493	3.936				
	30	10	155.6	239.3	417.8	1.320	50.42	.9903	.7936	.7525	.4466	3.929				
	31	100	218.6	356.8	437.0	1.122	42.62	.9387	.7576	.6946	.4314	3.743				
CURDFT = 5 amp cm ⁻²	32	500	207.1	341.5	266.6	.7466	30.03	.8425	.7534	.6125	.3841	3.174				
	33	1000	147.0	244.5	159.2	.5731	24.58	.8092	.7066	.5794	.3460	2.859				
	34	0	10	121.1	179.5	414.2	1.324	50.59	.9905	.7928	.7542	.4470	3.926			
	35	0	100	126.2	196.2	453.2	1.234	43.23	.9356	.7958	.7007	.4326	3.740			
	36	0	1000	103.9	162.0	160.7	0.5989	25.65	.8128	.7074	.5910	.3524				
	37	10	0	157.9	243.0	404.4	1.347	51.64	.9964	.7906	.7618	.4489	3.939			
	38	100	0	293.9	465.8	414.1	1.33	50.92	.9959	.7928	.7540	.4476	3.947			
Incident Power = 16.4 watt cm ⁻²	39	0	0	120.5	179.4	344.4	2.793	54.47	.9957	.7768	.7672	.4706	7.735			
	40	10	151.1	228.7	353.7	2.742	53.35	.9904	.7786	.7584	.4688	7.711				
	41	100	202.4	324.5	374.4	2.401	41.42	.9453	.7837	.7102	.4564	7.409				
CURDFT = 10 amp cm ⁻²	42	500	187.3	311.5	246.1	1.676	34.00	.8505	.7471	.6329	.4169	6.354				
	43	1000	152.5	252.8	159.6	1.311	28.10	.8116	.7069	.5986	.3817	5.737				
Incident Power = 1.64 watt cm ⁻²	44	0	0	164.2	254.9	518.7	.2457	45.82	.9984	.874	.7537	.4018	.8111			
	45	10	0	225.7	355.8	580.1	.2358	43.51	.9896	.8212	.7323	.3962	.8128			
	46	100	314.9	512.0	607.6	.1619	33.40	.9200	.8251	.6476	.3704	.7590				
CURDFT = 1 amp cm ⁻²	47	500	219.4	363.7	267.4	.1078	21.48	.8303	.7605	.5613	.3040	.6318				
	48	1000	159.6	264.1	169.9	.07839	16.67	.7929	.7125	.5254	.2641	.5649				

* The FORTRAN variables given in this table are defined in Table XIV. The estimated error in values of MAXROW is 1% or less. The values in the table are listed as they appeared in the computer program printout. Although the output values are generally inaccurate beyond the second decimal place, small differences between two corresponding output values for different values of input parameters will generally be accurate to the third or fourth decimal place.

Current-Voltage Curves of Device 8 Illuminated with Emissive Oxide Spectra.
(Devices are labeled according to device numbers in Table IV.)

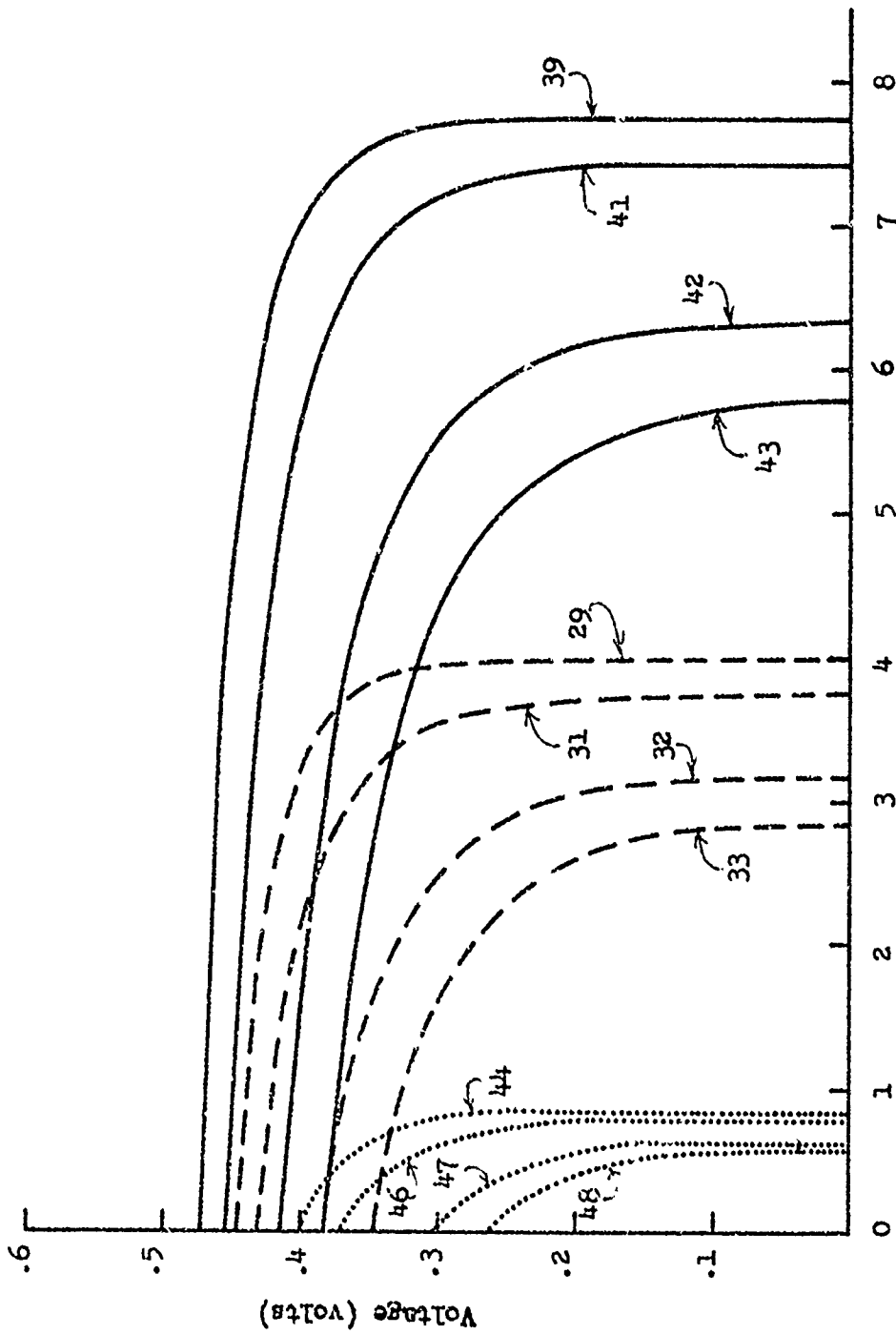


Figure 4. Current (AMPERES-CM⁻²)

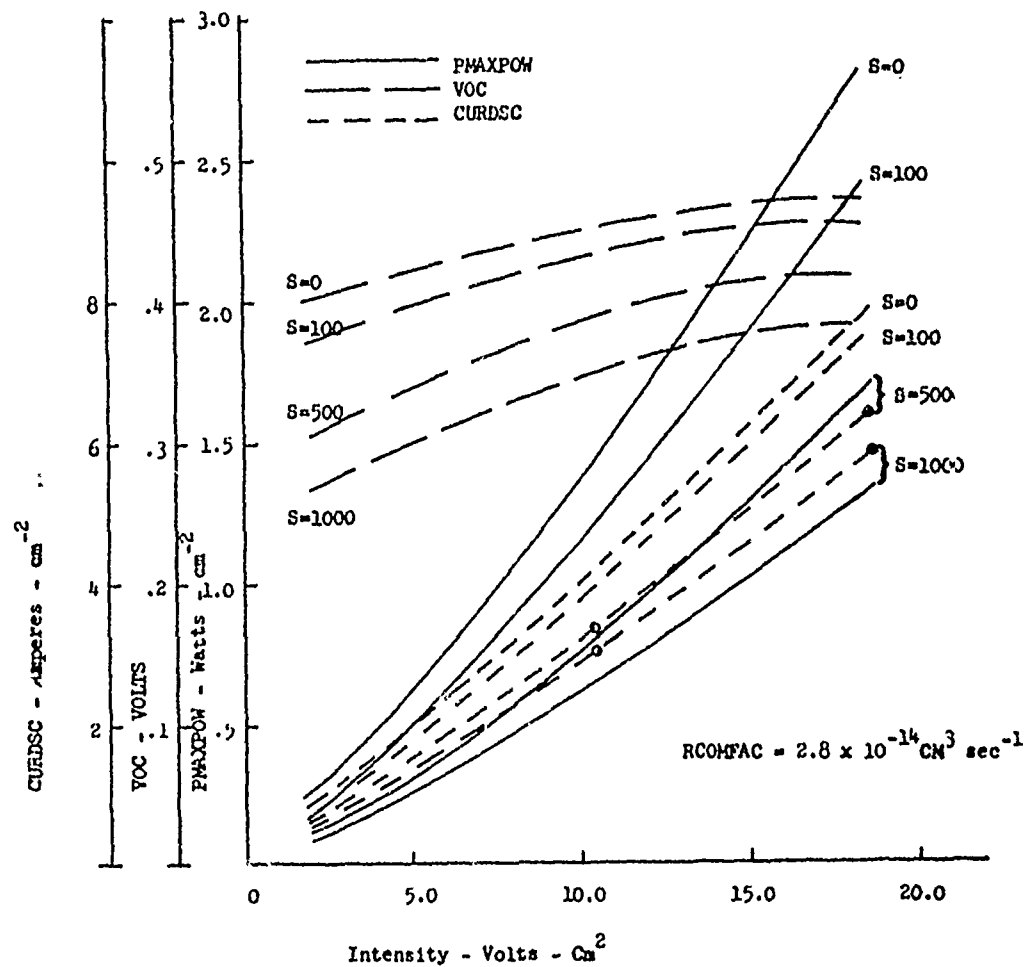
as V_{ST} is increased from 0 to 100 cm sec $^{-1}$. This is because the area of the illuminated surface is much greater than the area of the portion of the unilluminated surface between contacts.

For devices where the surface recombination velocity is the same on both the illuminated and unilluminated surfaces, the majority of the surface recombinations occur on the illuminated surface. However, it is expected that during processing it will be more difficult to maintain low surface recombination velocity on the unilluminated surface. Therefore, the total number of recombinations on either surface should be of comparable magnitude.

Some of the results of Table IV have been plotted in Figure 5. As would be expected the output power increases faster than a linear rate with increasing incident radiation intensity. However, because the radiative recombination increases as the square of the excess carrier concentration, the rate of rise in output power with increasing intensity is not as rapid as would be the case if all recombination occurred through trap sites.

The effect of recombination through trap sites is shown by the results summarized in Table V. These results are plotted in Figure 6. It is interesting to note that the open circuit voltages of devices 49 and 50 are greater than the open circuit voltage of device 29. This is because the recombination rate tends to vary linearly with the excess carrier concentration (m/τ) rather than with the square of the excess carrier concentration (rn^2). Therefore, as the device becomes thinner, the relative increase in excess carrier concentration and open circuit voltage will be greater.

-19-



Performance characteristics of cells optimized for radiation from an Er_2O_3 radiator. VSB-VST. See Table IV for device dimensions.

FIGURE 5

TABLE V
Optimum Dimensions and Output
Parameters of Devices with Finite Bulk Lifetimes*

$V_{SB} = V_{ST} = 0$ $L_1 = 25\mu M$ $R_{COMFAC} = 2.8 \times 10^{-4} \text{ cm}^3 \text{ sec}^{-1}$
 Incident Power = 9.2 watt cm^{-2} $CURDOPT = 5 \text{amp. cm}^{-2}$

Device	T_{AU}	L_N	L_P	X_O	P_{MAXPOW} (μM)	E_{FACELL} (watt- cm^{-2})	CF (%)	V_{OC} (volts)	$CURDSC$ (amp- cm^{-2})
29	∞	128.5	196.8	401.2	1.350	51.79	.7631	.4493	3.936
49	1000	116.0	169.3	289.3	1.272	50.66	.7461	.4517	3.774
50	100	54.95	81.71	78.70	1.024	48.08	.6973	.4578	3.207
51	10	31.03	53.48	50 ⁺	.6975	34.74	.6210	.3778	2.966

* The FORTRAN variables given in this table are defined in Table XIV. The devices are illuminated with on 1873°K Erbium Oxide Spectrum. The estimated error in [etc. (same as in Table IV.)
 +Device 51 is optimized under the constraint that the minimum attainable device thickness is $50\mu M$ because of limitations in fabrication technology.

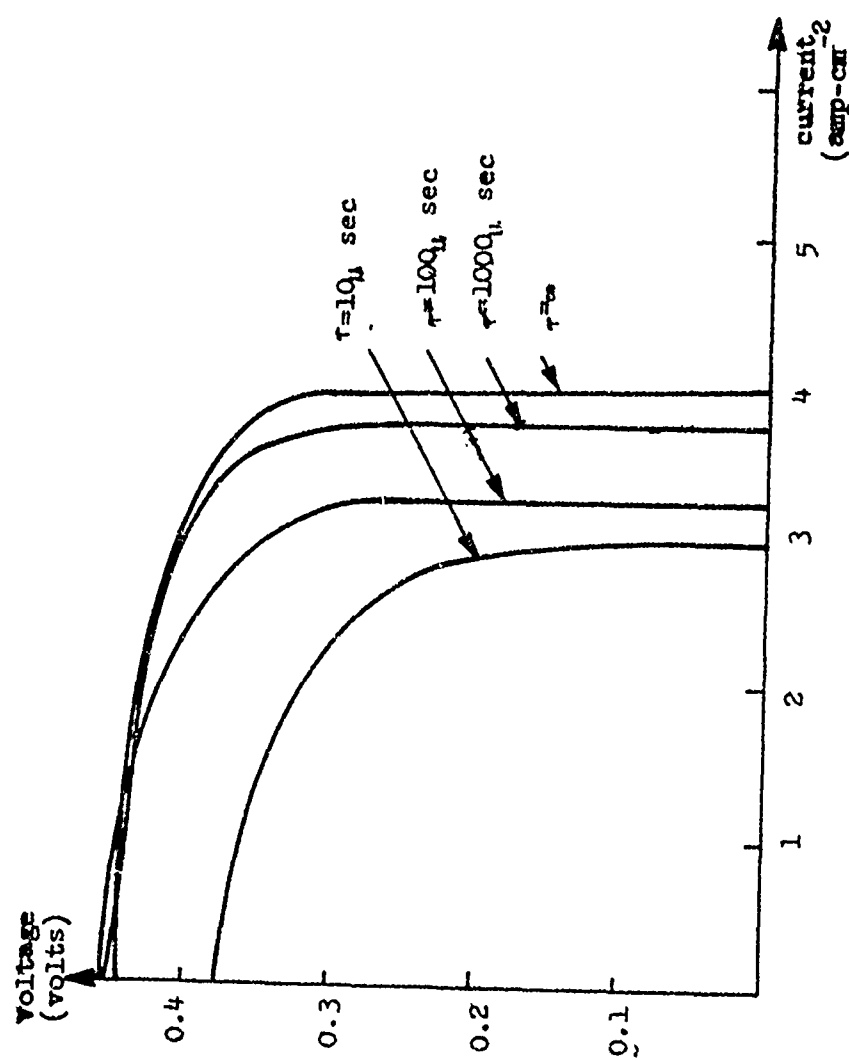


Figure 6. Current Voltage Curves of Devices with Finite Bulk Lifetimes

Consequently, the optimum thickness will tend to be smaller and the open circuit voltage will tend to be greater.

3. Radiation from a black body source

The results obtained from the ADOP program for devices illuminated with radiation from an 1873°K black body are summarized in Table VI. In general, for the same value of CURDMAX, the optimum device dimensions occurred at slightly larger values for black body radiation than for erbium oxide radiation. The conversion efficiency is also lower because a larger portion of the radiation energy is in unfavorable portions of the energy spectrum. Device 52 (Table VI) has a conversion efficiency of 12.7% when illuminated with 1873°K blackbody radiation while device 29 (Table IV) has a conversion efficiency of 14.7% when illuminated with 1873°K Er_2O_3 radiation. In both cases the value of CURDOPT is 5.0 amps cm^{-2} .

TABLE VI
Optimum Dimensions and Output Parameters of Devices

Illuminated with 1873K Black Body Spectrum*
 LI = 25 μm Incident Power = 9.8 Watt cm^{-2} CURDOPT = 5.0 amps cm^{-2}
 RCOMFAC = 2.8×10^{-14} $\text{cm}^3 \text{sec}^{-1}$

Device #	VSB (cm sec^{-1})	YST (cm sec^{-1})	LN (μm)	LP (μm)	XO (μm)	PHXPOW (watt cm^{-2})	PHACELL (%)	ETAAB	CF	VOC (volts)	CURDSCA (amp cm^{-2})
52	0	0	150.3	224.3	508.5	1.241	50.07	.9935	.7508	.4416	3.730
53	10	10	170.1	264.7	520.2	1.214	48.85	.9861	.7532	.4395	3.714
54	100	100	234.1	377.8	530.8	1.029	41.30	.9258	.7552	.4259	3.496
55	500	500	221.2	366.6	321.1	.6705	28.81	.8184	.7052	.6104	2.886
56	1000	1000	157.9	262.7	179.5	.5070	23.65	.7927	.6496	.5760	2.573
57	0	10	152.5	229.3	518.0	1.216	48.96	.9861	.7528	.7451	4.398
58	0	100	154.3	234.2	526.0	1.040	41.77	.9262	.7544	.6968	3.762
59	0	1000	166.8	265.3	375.0	.0540	21.20	.6717	.7204	.5875	4.272
60	10	0	179.1	286.2	510.9	1.239	49.96	.9936	.7514	.7518	3.493
61	100	0	291.3	477.5	519.9	1.226	49.33	.9928	.7532	.7450	2.420
											3.733
											3.739

-23-

* The FORTRAN variables given in this table are defined in Table XIV. The estimated error in values of PHXPOW is 1% or less. The values in the Table are listed as they appeared in the computer program printout. Although the output values are generally inaccurate beyond the second decimal place, small difference between two corresponding output values for different values of input parameters will generally be accurate to the third or fourth decimal place.

II. EXPERIMENTAL INVESTIGATIONS

A. Introduction

The discussion of the experimental work will consist of the following: (1) a brief description of the device fabrication process; (2) a detailed description of investigations involving the fabrication process; (3) a discussion of the performance of devices that have been fabricated, and (4) a listing of the deficiencies which exist in devices that have been fabricated and a description of tests that have been carried out to isolate these deficiencies and measure their effects.

B. Description of Device Fabrication Process

The steps involved in fabricating a TPV cell are given below.

1. An intrinsic germanium wafer is chemically polished on both sides.²
2. An insulating film is deposited on both sides of the wafer.
3. A pattern for the formation of the n contact is etched in the insulator on one side of the wafer.
4. Metal(s) for the n contact is vacuum evaoprated on the wafer.
5. The metal(s) is etched so that it covers only the portion of the wafer on which the insulator has been etched. (See Figure 7.)
6. A pattern for the formation of the p contact is etched in the insulator.
7. Metal(s) for the p contact is vacuum evaporated on the wafer.

8. The metal(s) is etched so that it covers only that portion of the wafer on which the insulator has been etched for the p contact.

9. The contact metals are alloyed to the germanium. (See Figure 8.)

During the course of the experimental work some devices were fabricated according to the above procedure. A number of variations in this procedure were investigated, and a variety of insulating films and contact metals were investigated.

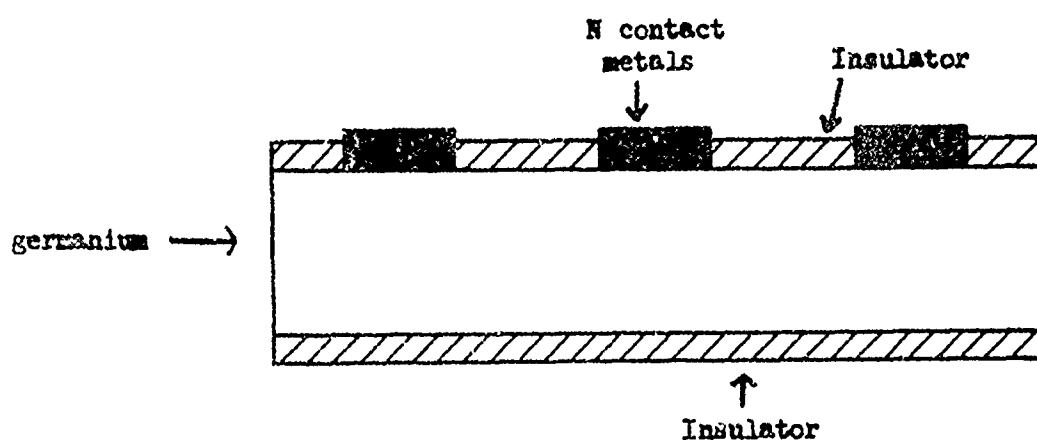


Figure 7. Partially Fabricated p-i-n Thermophotovoltaic Cell

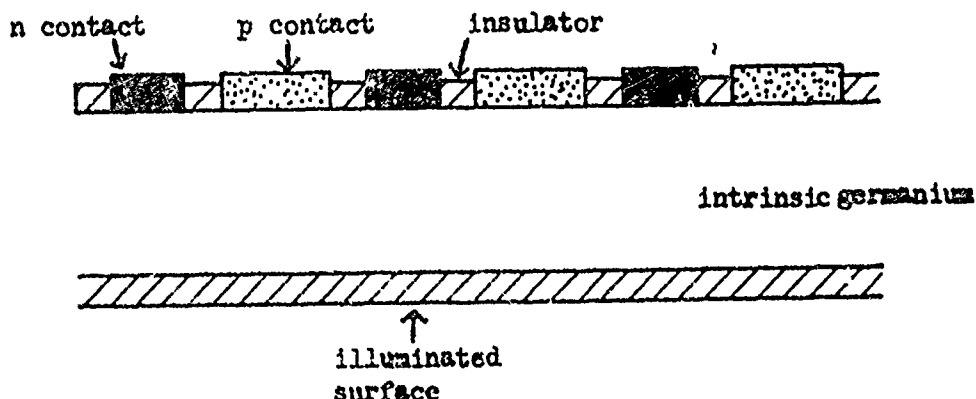


Figure 8. Completely Fabricated p-i-n Thermophotovoltaic Cell

C. Experimental Investigations of the Fabrication Process

1. Insulator deposition

The insulators which have been investigated are pyrolytically deposited silicon dioxide and vacuum deposited aluminum oxide.

Silicon dioxide deposition.-- It is desirable to carry out device processing at the lowest possible temperature in order to prevent diffusion of lifetime destroying impurities into the germanium bulk. Therefore, an investigation was carried out in order to determine the lowest possible temperature at which the silicon dioxide could be deposited. A reasonably fast deposition (900 \AA/min) could be obtained at a temperature as low as 310°C .

A method of device fabrication was proposed in Report No. 1¹ in which the p contact was formed before the n contact. Aluminum was to be used for the p contact. After the aluminum was deposited, etched and alloyed, silicon dioxide was deposited on top of the aluminum. Windows for n contacts were then etched in the silicon dioxide, and metals (gold and antimony) for the n contact were subsequently evaporated and alloyed. The necessity of etching the n contact metals was to be eliminated because of the insulating layer between the aluminum and the n contact metals.

The results of attempts to fabricate devices with the above described procedure were as follows: In cases where the silicon dioxide layer was deposited on top of the aluminum contact at 360°C , the p and n contacts were invariably shorted. Furthermore, the silicon dioxide invariably cracked on the aluminum once the thickness of the silicon dioxide exceeded 2000 \AA . Devices for which the silicon dioxide was deposited at 425°C were occasionally workable.

Aluminum oxide deposition.-- An investigation was carried out to determine if vacuum evaporated aluminum oxide could be used as an insulating layer between contacts. It was observed, however, that, while aluminum oxide appeared to cover the top of the aluminum contact well, it did not cover the contact edges.

Photoresist problems with SiO₂ films.-- The positive photoresist AZ-1350* is generally used during the device fabrication. When this photoresist is used on pyrolytically deposited silicon dioxide, it is necessary to take certain precautions.

First of all, the developer which is normally used with this photoresist (AZ-1350 Developer*) contains an abundance of sodium ions. Since silicon dioxide is highly permeable to sodium ions, and since it is feared that these ions will have a detrimental effect on the surface recombination velocity, it is desirable to use the developer XP-7110-1.*

Secondly, AZ-1350 has a tendency not to stick to pyrolytically deposited silicon dioxide, and, therefore, it is necessary to take extra precautions to insure adhesion.

2. Contact formation

In order to avoid excessive leakage of minority carriers through the contacts, it is necessary that the contacts be very heavily doped and fairly thick. The requirement of low temperature processing rules out the use of high temperature diffusion techniques because of the danger of diffusion of lifetime destroying impurities into the germanium bulk. Heavily doped contacts can be obtained with alloying techniques, but in order to obtain sufficiently thick regrowth regions, it is necessary either to alloy at high temperatures or to deposite rather thick films

*Mfg. by Shipley.

of contact metals (1μ or thicker). Experimental investigations have shown that the thickness of vacuum deposited films is limited because of the effects of surface tension in the films. The increased surface tension of thick films has two adverse effects: (1) There is a tendency for the films to ball up or develop craters during the alloying process. (2) The adhesion of the films is poorer.

n contacts

Kim⁴ has investigated several combinations of metals for forming alloyed n contacts and has found that the best results were obtained when gold was used as a carrier with arsenic and antimony being used as dopants. For this reason investigations were carried out in which these metals were to be used to form alloyed n contacts. It was discovered that vacuum deposited films of gold and antimony adhered very poorly to germanium, and, therefore, it was impossible to etch these films without removing them from the germanium. Because of this adhesion problem, several attempts were made to build a device without having to etch the gold-antimony film. The first of these attempts is described on page .

The second attempt was identical to the first attempt except that the position of silicon dioxide on the aluminum contact pattern was omitted. Instead, a second layer of aluminum was evaporated and etched to cover the first layer of aluminum. After the gold-antimony film was evaporated, it was alloyed to the germanium at a temperature below the aluminum-germanium eutectic . It was hoped that the unalloyed aluminum film would not be affected by the gold-antimony layer on it during the alloying process. Then the alloyed gold-antimony film (which would stick to the germanium during the photo etching process) could be etched to separate the n contact

from the p contact. It was evident, however, that the gold-antimony film had interacted with aluminum film during the alloying process.

The proposed steps in the third attempt to fabricate a device were as follows: (1) Silicon dioxide would be deposited on both sides of a germanium wafer. (2) A pattern would be etched in the silicon dioxide on one side of the wafer through which the n contact would be formed. (3) Gold and antimony would be evaporated and alloyed to form the n contact. (4) The gold-antimony film would be etched so that it would remain only in those regions of the device on which the n contact pattern had been etched through the silicon dioxide. (5) A p contact pattern would be etched. (6) An aluminum film would be deposited and etched so that it would cover only the p contact region. (7) The aluminum would be alloyed to the germanium.

After the gold-antimony film had been alloyed [step (3)], however, large areas of balled-up gold-antimony alloy formed on the silicon dioxide. When step (4) was carried out, it was observed that the photoresist broke down before the thick balled-up regions could be completely etched.

An unsuccessful attempt was made to improve adhesion of gold to germanium by evaporating a mixture of gold and germanium simultaneously on a germanium wafer.

Eventually it was discovered that gold would adhere extremely well to germanium if the gold were evaporated immediately after the germanium surface had been subjected to an argon ion etch.*

* The ion etch is carried out at an argon pressure ranging from 50 microns to 10 microns while the vacuum system is pumping down the pressure. The duration of the ion etch is about 30 sec. The germanium wafer is in good electrical contact with a cathode that is maintained at a voltage of 600 volts D.C.

Several methods of "etching" the gold antimony films were investigated. These methods are described below:

Chemical etching.-- While chemical etching is procedurally complicated, it invariably produces sharp etches and can be used with relatively thick vacuum deposited films.

Ultrasonic "etching"-- Although gold sticks very well to ion etched germanium, it does not stick at all to silicon dioxide. Therefore step 5 of the procedure outlined in section B (page 24) can be carried out by removing the gold-antimony film from the silicon dioxide with a rigorous ultrasonic cleaning. Although this method of "etching" is procedurally simple, it has two disadvantages: (1) It does not produce as sharp a pattern as chemical etching. (2) It tends to become less satisfactory as the gold-antimony film becomes thicker. This is because the adhesion of the film to germanium becomes poorer.

Photoresist lift-off "etching"-- A third method of "etching" can be carried out as follows: (1) A photoresist pattern is developed on the wafer. (2) The metal film is deposited. (3) The photoresist and the metal film on top of it are stripped from the wafer, leaving a metal pattern which complements the photoresist pattern.

This method of etching has three disadvantages: (1) It does not produce as sharp a pattern as chemical etching. (2) It does not work for films that are too thick. (The photoresist won't lift off thick films.) (3) It is inherently dirtier than chemical or ultrasonic etching.

The advantage of photoresist lift-off etching is that the problem of etching the second metal contact pattern without attacking the first is eliminated.

A device was built using lift-off etching techniques. The processing steps were as follows: (1) Silicon dioxide was deposited on both sides of a wafer. (2) Both p and n contact patterns were etched in the wafer. (3) A photoresist pattern was developed which left only the p contact region uncovered. (4) An aluminum film was deposited. (5) The photoresist and the aluminum film above it were stripped from the wafer. (6) A photoresist pattern was developed which left only the n contact region uncovered. (7) Gold and antimony were deposited after an ion etch. (8) The photoresist and the gold-antimony film above it were stripped from the wafer.

Arsenic doped contacts.-- Investigations were carried out in which arsenic was used with gold or gold and antimony to form alloyed n contacts. Two noteworthy observations were made: (1) Arsenic-gold and arsenic-antimony-gold film tended to stick fairly well to germanium, provided that the arsenic was evaporated first. However, the films did not stick as well as gold antimony films of comparable thickness which had been deposited after an argon ion etch. (2) Alloyed arsenic-gold films tended to ball up much more readily than arsenic-antimony-gold films of comparable thickness.

Other combinations of metals have been investigated for n contacts. These investigations are discussed later.

p contacts

Aluminum has been thoroughly investigated as material for forming p contacts because of its very high solid solubility in germanium.

Thick films of aluminum (of the order of $10 \mu\text{m}$) have been investigated because of the need to form thick germanium regrowth regions during

the alloying process. Because of the long time required to etch these films, the photoresist would break down, and pin holes would develop in the aluminum film. Experiments were conducted with various etchants and etching techniques to eliminate this problem. It was determined that photoresists would hold up satisfactorily if the film was etched in warm aluminum etch* (approximately 40°C).

Experiments have been conducted to determine if the adherence of aluminum films could be improved by an ion etch, (although aluminum films generally stick well without ion etches). The results indicate that the adherence of aluminum is improved slightly by an ion etch.

Other metals and combinations of metals have been investigated as materials for forming p contacts. The results of these investigations as well as the results of more detailed investigations of aluminum will be discussed in the following section.

Alloying

An extensive series of investigations was carried out in which various metal films and combinations of metal films were tested for possible use as p or n contacts. The metallic films were alloyed to the germanium at various temperatures and were angle-lapped and stained. The quality of the films was judged on the basis of the smoothness of the crystal regrowth region in the germanium.

Junction staining solution.-- Some preliminary tests were carried out in order to select a suitable junction staining solution. Aluminum balls were alloyed to germanium substrates to form thick heavily doped regrowth regions in the germanium. The substrates were lapped through the alloyed region and stained with various solutions. The best results were

*The composition of aluminum etch is given in Table VIII.

obtained with a 30 second stain in a solution consisting of 20 parts HF to one part HNO_3 .

Alloying technique.-- All metallic films were vacuum deposited on chemically polished germanium substrates which had been cleaned ultrasonically in methanol, acetone and trichlorethylene and exposed to an argon ion etch.

The alloying was done in an alloying system in which the substrate was placed between two carbon heater strips. The heater strips could be heated independently, and thus the sample could be alloyed in a temperature gradient. The spacing between heater strips was about a half millimeter. The sample was placed on the lower heater strip with the surface on which the metallic film had been evaporated facing upward. The temperature of the upper strip was maintained about 100°C higher than that of the lower strip.* The alloying temperatures given in the following discussions are those of the lower substrates.

The samples were heated at a rate of about $10^{\circ}\text{C sec}^{-1}$. A cooling rate of about $5^{\circ}\text{ C sec}^{-1}$ was begun immediately after the alloy temperature had been reached. All alloying was done in hydrogen.

Aluminum films.-- Aluminum films approximately one micron thick were deposited on germanium substrates. The films were alloyed at temperatures of 450°C , 500°C and 700°C . The samples were angle-lapped and stained. In the samples which were alloyed at 500°C and 700°C , the regrowth regions were extremely irregular, and there was no perceptable

*According to EerNisse⁵ the regrowth region in the germanium substrate tends to be smoother when the temperature of the alloy melt is maintained above that of the germanium substrate.

regrowth in the sample which was alloyed at 450°C.

There was also a tendency for craters to form on the alloyed aluminum film. There was no perceptable regrowth in germanium regions under these craters.

Indium films.-- An indium film approximately one micron thick was deposited on a germanium substrate and alloyed at 650°C. The film balled up badly during the alloying process, and regrowth was visible only under the balled up regions.

Aluminum on indium films.-- Indium films (approximately one micron) followed by aluminum films (approximately one micron) were deposited on germanium substrates. The films were alloyed at 650°C, 500°C, 450°C and 350°C. The regrowth region of the film alloyed at 650°C was fairly smooth, but it got progressively more irregular for the films alloyed at 500°C and 450°. The regrowth region was quite smooth for the film alloyed at 350°C. This was probably due to the fact that the alloying temperature was below the germanium-aluminum eutectic (424°C), and, therefore, the aluminum film did not liquify during the alloying process.

The "cratering" effect described in the discussion of aluminum films also occurred for these films. The craters tended to get progressively smaller at lower temperatures and were imperceptable for the film alloyed at 350°C.

Antimony on gold films.-- Gold films (approximately one micron) followed by antimony films (approximately one half micron) were evaporated on germanium substrates. The films were alloyed at 700°C and 525°C. The films balled up badly during the alloying processes, and regrowth was visible only under the balled up regions.

Antimony films.-- About three microns of antimony were evaporated on a germanium substrate and alloyed at a temperature of 700°C. The antimony balled up very badly during the alloying process, and no regrowth was visible in the germanium.

Tin-antimony-tin films.-- Some samples were prepared with a vacuum deposited film consisting of two layers of tin with a layer of antimony between them. The first and second layers of tin were approximately one half and one micron thick, and the antimony layer was approximately one half micron thick. The samples were alloyed at 475°C and 650°C. The regrowth regions were quite smooth and regular.

Conclusions.-- The most promising junctions for p contacts were obtained with the indium-aluminum films. The most promising junctions for n contacts were obtained with the tin-antimony-tin films. An attempt was made to fabricate a device using these films. It was discovered, however, that the adhesion of the films was not good enough.

An attempt was made to form tin-antimony-tin contacts on a device by alloying the film before etching it. Silicon dioxide was deposited on both sides of a wafer and was etched on one side to form an n contact pattern. A tin-antimony-tin film was evaporated and alloyed. But during the alloying process, the film balled up badly on the silicon dioxide, and apparently the surface tension created in the balled up regions on the silicon dioxide was large enough to cause the film to also ball up in the contact region.

Further investigations need to be carried out to determine the maximum thicknesses of indium-aluminum films and tin-antimony-tin films that will stick well enough to germanium to withstand ultrasonic cleaning and photoprocessing.

Contact buildup

Since the thermophotovoltaic cell is designed for very high intensity illumination, rather large currents will be collected at the contacts; and, consequently, it is necessary that the resistance in the contact fingers be quite low. Therefore, investigations were carried out in which the resistance of the contact fingers was reduced by plating relatively thick (10-20 micron) films of gold on the contacts.

Attempts were made to plate gold directly on the alloyed aluminum and gold-antimony contacts of a completed device. The gold plating on the aluminum did not stick at all. The gold plating on the gold-antimony contact appeared to stick reasonably well, but the plating on the gold-antimony fingers bridged over to the aluminum fingers in several places.

The following method of building up the contacts satisfactorily eliminated the bridging over problem and permitted a buildup of both aluminum and gold-antimony contacts: (1) Very thin chrome and gold films were evaporated over the contact surface of the device. (2) A relatively thick gold film was electroplated on the vacuum deposited gold film. (3) The chrome-gold film was then etched to separate the P and N contacts. The chrome film was evaporated to form an adhesive layer with the aluminum; and the gold film was evaporated subsequently without breaking vacuum in order to prevent oxidation of the chrome film and thus insure the adhesion of the electroplated gold film. It is desirable to build up the contacts with electroplated rather than evaporated gold, because thick films of evaporated gold would produce an appreciable amount of surface tension. This surface tension would cause stresses in the germanium which could significantly reduce lifetime.

3. Fabrication problems

Compatibility of etchants and processing chemicals.-- A variety of chemicals and etchants are used in the process of fabricating a device. Some of the etchants which are quite satisfactory for etching the metal or insulator for which they are meant will attack other areas of the device. The fabrication process must be carried out in such a way that this doesn't happen. Table VII lists some of these chemicals and etchants and their effects on metals and insulators that are used in the fabrication process. The compositions of the etchants listed in Table VII are given in Table VIII.

Problems with gold contacting aluminum.-- The following process was used to fabricate the devices which were evaluated in the tests in section II-D: (1) Silicon dioxide was deposited on both sides of a wafer. (2) A pattern for n contacts was etched in the silicon dioxide. (3) A gold-antimony-gold* film was deposited and etched to form the n contact. (4) A pattern for p contacts was etched in the silicon dioxide. (5) An aluminum film was deposited and etched to form the p contact. (6) The contact metals were alloyed to the germanium.

A problem occurred in step (5). Normally it is necessary to heat the device to a temperature of about 100°C for a period of about 30 minutes during the photoetching process. This heating period caused the aluminum to react with the gold. A method of photoprocessing without heating the device was developed in order to eliminate this effect.

* The film consisted of two layers of gold with a layer of antimony between them.

TABLE VII

Effect of Chemicals and Etchants on Metals and Insulators

Chemical & Etchants	Metals & Insulators									
	Germanium	Silicon Dioxide	Aluminum Oxide	Aluminum	Indium	Gold	Antimony	Arsenic	Tin	Chrome
Silicon Dioxide Etch	4	1	1							
Aluminum Etch	4	4	1	1	1	4	3			
Gold Etch	2	4		1A		1	4			
Antimony Etch	1	4		2	1	1	1	1	1	
Chrome Etch		4				4			1	
Nitric Acid	4	4		2	1		2	1		
J-100	4	4	4	4		4	3			
Water				2A						

1. Etches rapidly.
- 1A. Does not attack aluminum but lifts off the aluminum by attacking the germanium surface under the aluminum film.
2. Etches slowly
- 2A. Causes flaking of film after several days immersion.
3. Has a discoloring effect.
4. Has no apparent effect.

TABLE VIII

Etchants used in Device Fabrication

Silicon Dioxide Etch:	104 ml Hydrofluoric acid 454 gm Ammonium Fluoride 682 ml Water
Aluminum Etch:	380 ml Phosphoric Acid 15 ml Nitric Acid 75 ml Acetic Acid 25 ml Water
Gold Etch:	27 gm Iodine 60 gm Potassium Iodide 600 ml Water
Antimony Etch:	3 parts Nitric Acid 1 parts Hydrochloric Acid 6 parts Water
Chrome Etch:	27 gm Cerium Sulfate 100 ml Nitric Acid 400 ml Water

4. Heat sink fabrication and device mounting

A photograph of a finished device mounted on a heat sink is shown in Figure 9. The interior of the heat sink is hollow. Cooling water enters and exits through the openings at opposite ends of the heat sink. The portion of the heat sink under the device is milled to a thickness of 1/16 inch. The milled surface is left unfinished to facilitate the conduction of heat between the surface and the circulating water. The heat sink is anodized in sulfuric acid to form an insulating layer of aluminum oxide approximately $5 \mu\text{m}$ thick. The milled out portion is sealed at the bottom with an aluminum block which is epoxied on with stycast 2850FT*. Banana jacks are soldered on two copper contact plates which are epoxied on opposite sides of the heat sink with Stycast 2850FT*.

The device is epoxied to the heat sink with Stycast 2850FT* used with the catalyst 24 LV. First of all, the device is mounted (the illuminated surface facing downward) on a glass slide with beeswax. The glass slide provides mechanical support. The device is then epoxied to the heat sink with the p and n contact pads extended over opposite edges of the heat sink. After the epoxy has cured the glass slide is removed by melting the beeswax, and the beeswax is removed with trichlorethylene. Finally the contacts on the device are soldered to the contact plates with Indalloy Solder #8 used with Flux #2.**

* Manufactured by Emerson Cumming.

** Manufactured by the Indium Corporation of America.

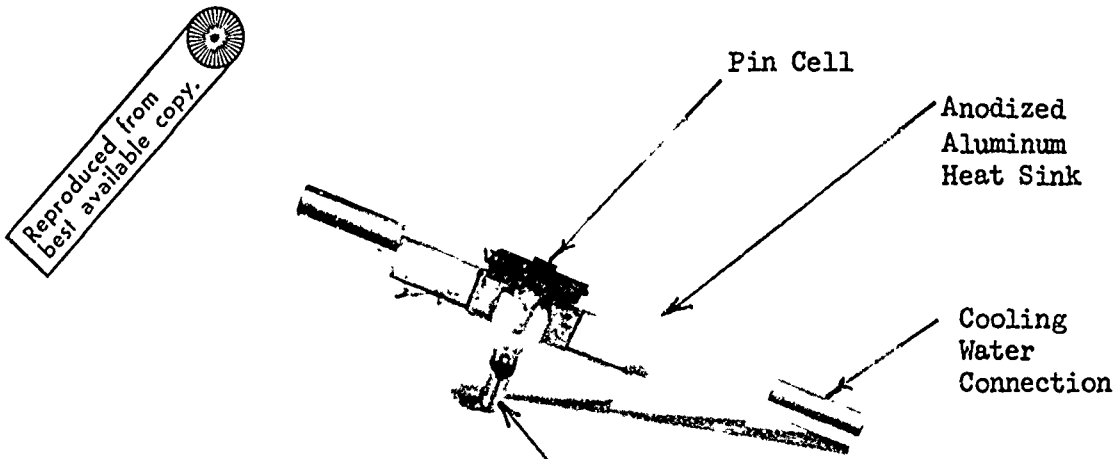


Figure 9 Electrical Connection

p-i-n Cell Mounted on Water
Cooled Heat Sink

5. Evaluation of heat sink performance.

The following experiment was carried out to estimate the degradation in the performance of heat-sunked cells due to the heating effect of the $9.95 \text{ watt-cm}^{-2}$ illumination source: A shutter was inserted between the cell and the illumination source to prevent heating of the cell. The I-V characteristics of the cell were monitored on a curve tracer. A series of traces on the curve tracer was photographed immediately after the shutter was removed. The effect of heating could be determined by observing the degradation in the I-V characteristics on the photograph of the traces.

In cases where there was no fluid circulating through the heat sink, a very significant degradation occurred in the cell performance. In cases where there was water circulating through the heat sink, however, the degradation was practically imperceptable.

D. Performance of Fabricated Devices

Some devices were fabricated with the process outlined pages 24 and 25. The open circuit voltages of each device was measured in a sample holder in which the illuminated surface was faced downward on a glass slide. A tungsten lamp illuminated the sample through the glass slide with an incident intensity of 0.7 watts/cm². No measurements were made to determine what percentage of the incident light was absorbed by the sample.

The results of the open circuit voltage measurements are shown in Table IX. The Table also lists the unique characteristics of each device.

Two note worthy observations can be made from the data in Table IX:
(1) The quality of the device generally improves as the film thickness (especially the thickness of the n-contact films) is increased. (2) The quality of devices alloyed at temperatures at or above 550°C is better than that of those alloyed below 550°C.

The open circuit voltage of device #4 was measured again with the 0.7 watt/cm² tungsten lamp being replaced with a 9.95 watt/cm² tungsten lamp. The measured open circuit voltage was 0.28 volts.

Devices #1, 4 and 6 in Table IX were mounted on heat sinks. Because of problems encountered with breakage during processing, the active area of device #1 was reduced to 0.6 cm x 0.55 cm. Problems were encountered with the adhesion of electroplated gold films on devices #1 and 4. As a result the performance of these devices was significantly degraded after they were mounted on the heat sinks.

The I-V characteristics of device #6 are shown in Figure 10. The 9.95 watt/cm² illumination source is used. The short circuit current

TABLE IX
Open Circuit Voltage Output of Fabricated Devices
0.7 w/cm² Tungsten Illumination

Device #	Active area (cm x cm)	Total Thickness of Gold Films (Å)	Thickness of Antimony Film (Å)	Aluminum Film (Å)	Alloying Temperature (°C)	Open Circuit voltage (volts)
1*	0.6 x 1.5	300	300	1500	450	0.10
2	0.6 x 1.5	250	250	1500	450	0.06
3	0.55 x 0.30	1000	750	6000	450	0.12
4*	0.55 x 0.30	1000	750	6000	550	0.19
5	0.55 x 0.30	500	250	12000	550	0.165
6*	0.55 x 0.30	500	250	12000	550	0.16
7	0.5 x 0.30	500	250	6000	700	0.14

* Mounted on heat sinks

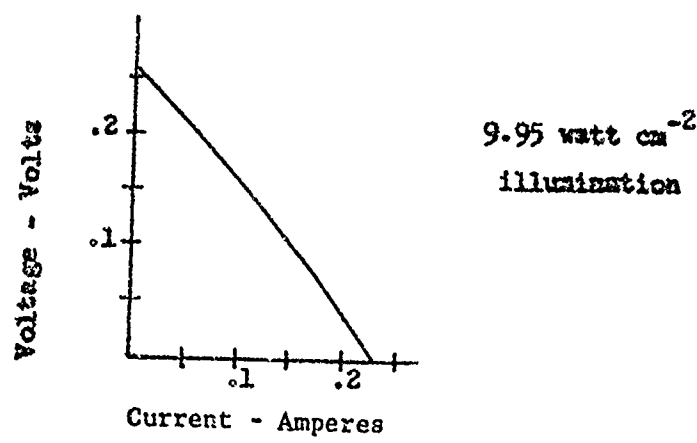


Figure 10. Voltage Curves for
Device #6 (See Table IX)

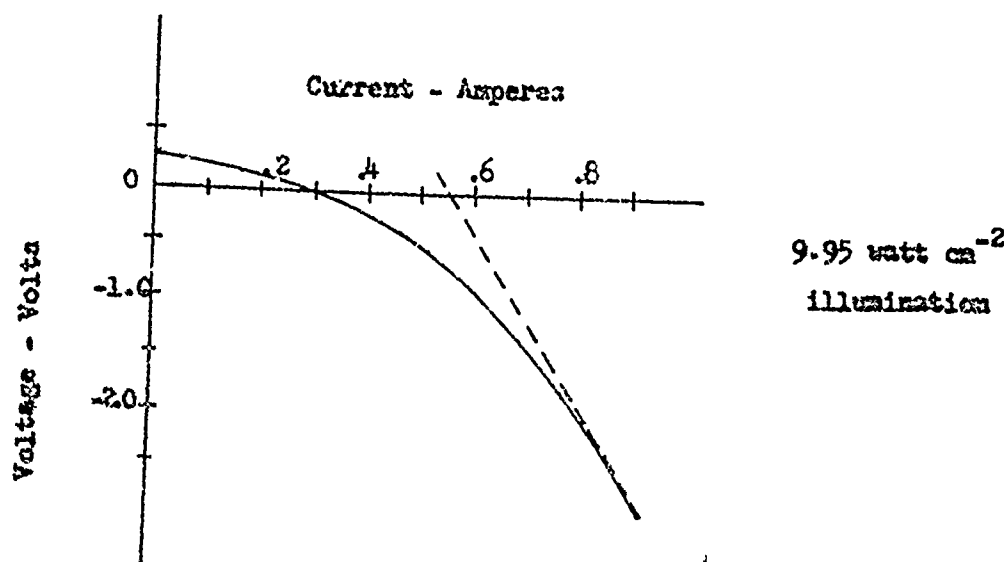


Figure 11. Current - Voltage Curve for Device #6
Reverse Bias Applied (See Table IX).

obtained is 240 ma. Since the active area of the device is $0.55 \text{ cm} \times 0.30 \text{ cm}$ (See Table IX), the short circuit current collected per unit area is 1.5 amp cm^{-2} .

An attempt was made to estimate the maximum attainable short circuit current. A reverse bias was applied to the device, while it was illuminated by the 9.95 watt cm^{-2} source. The reverse characteristics appeared to approach an asymptote. (See Figure 11.) The asymptote intersected the current axis at 550 ma. This current is presumably the maximum collectable current of the device. The current collectable per unit area for the $0.55 \text{ cm} \times 0.30 \text{ cm}$ device is 3.3 amp cm^{-2} .

E. Investigation of Deficiencies in Devices

The deficiencies in the performances of the devices that have been fabricated can be attributed to any combination of the three following factors: (1) excessive bulk recombination; (2) excessive surface recombination; (3) faulty contacts. The following discussion describes how the relative importance of each of these deficiencies is evaluated.

1. Contacts deficiencies

A series of samples was prepared according to the following procedure: (1) Silicon dioxide was deposited on both sides of a polished intrinsic germanium wafer. (2) A pattern of dots was etched through the silicon dioxide on one side of the wafer. (3) An aluminum film was deposited over

half the surface on which the dot pattern had been etched.

(4) Metal films for n contacts were deposited on the other half of the wafer on which the dot patterns had been etched. (5) The aluminum and n contact films were etched to form a complementary pattern to the silicon dioxide pattern. (I.e., the metal films patterns consisted of dots which covered the areas of the surface on which the silicon dioxide film had been etched.) (6) The aluminum and n contact films were alloyed simultaneously.

The open circuit voltage of the devices fabricated according to the above procedure was measured while the unprocessed surface of the device was illuminated with the 0.7 watt/cm² source. The testing procedure was exactly the same as that used to obtain the results shown in Table IX. The results of the measurements are summarized in Table X. The following conclusions can be drawn from these results: (1) In general the open circuit voltages obtained for devices with the arsenic-doped contacts is better than that obtained for devices without arsenic-doped contacts. (2) The open circuit voltage seems to hit an upper limiting value of 0.20 volts.

2. Lifetime damage due to silicon dioxide deposition

A series of tests was carried out to evaluate the effect of silicon dioxide deposition on the bulk and surface lifetime of devices. Three germanium strips were cut from an intrinsic wafer which had been polished on both sides. Silicon dioxide was deposited on one side of one strip and on both sides of another. Four gold contacts were then evaporated on each strip to form the type of structure shown in Figure 12. The portion of the contact on the rough edge was for the purpose of forming a good ohmic contact; and the portion of the contact on the polished

TABLE X

Open Circuit Voltage Output of Dot-Pattern Devices

Device #	Thickness of Aluminum Film (A)	n Contact Material*	Thickness of n Contact Material Film (R)	Alloying Temperature (°C)	Open Circuit Voltage (volts)
1	4500	Au	360	435°C	0.125
		Sb	400		
		Au	120		
2	4500	Au	360	520°C	0.17
		Sb	400		
		Au	120		
3	4500	As	130	435°C	0.195
		Sb	130		
		Au	700		
4	4500	As	130	520°C	0.20
		Sb	130		
		Au	700		
5	4500	As	200	435°C	0.20
		Sb	500		
		Au	10,000		
6	4500	As	200	435°C	0.15
		Sb	500		
		Au	3,000		
		Sb	20,000		

* The n contact films for a device are listed in the order in which they were evaporated.

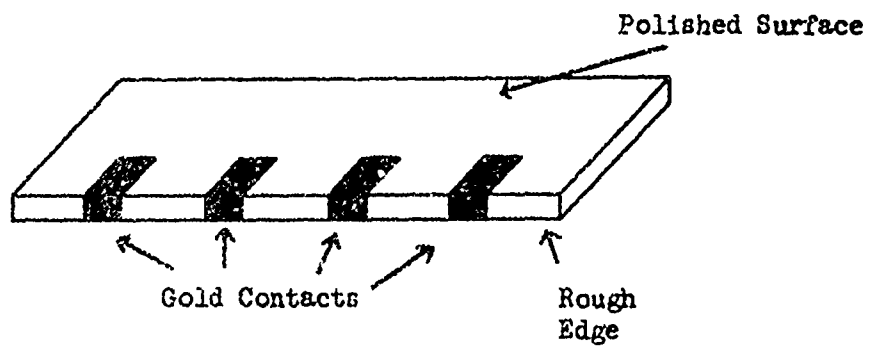


Figure 12. Sample Used to Test Effect of Silicon
Dioxide Deposition on Lifetime

surface was for making contact with a probe.

The sample was illuminated, and the excess carrier concentration due to the illumination was measured by measuring the conductivity of the substrate. (See Figure 13.) Since the gold contacts were not perfectly ohmic, the conductivity was measured by a four point probe technique. A fixed current flowed through the outer probes, and the voltage drop was measured across the inner probes with a high impedance volt meter. Since the germanium substrates were intrinsic, the ratio of excess carrier concentration to intrinsic carrier concentration was given by the ratio of the voltage drop without illumination to the voltage drop with illumination.

The results of the measurements are summarized in Table XI. The test fixture and illumination source are the same as those used to obtain the results shown in Tables IX and X.

The following conclusions can be drawn from the results in Table XI:

- (1) The deposition of silicon dioxide appears to degrade the bulk and/or surface lifetime.
- (2) The silicon dioxide film enhances the absorption of useful illumination.
- (3) The effect of depositing silicon dioxide on both sides of the wafer is not significantly different from the effect of depositing it on one side only.

3. Determination of the dominant source of recombination

Theoretical investigations have shown that surface recombination velocity is smaller for accumulated or depleted surfaces than for flat band surfaces. An experiment was carried out in which the surface recombination velocity of a germanium substrate was varied by varying the surface potential. The substrate was prepared like the sample shown in Figure 12 with silicon dioxide films deposited on both sides.

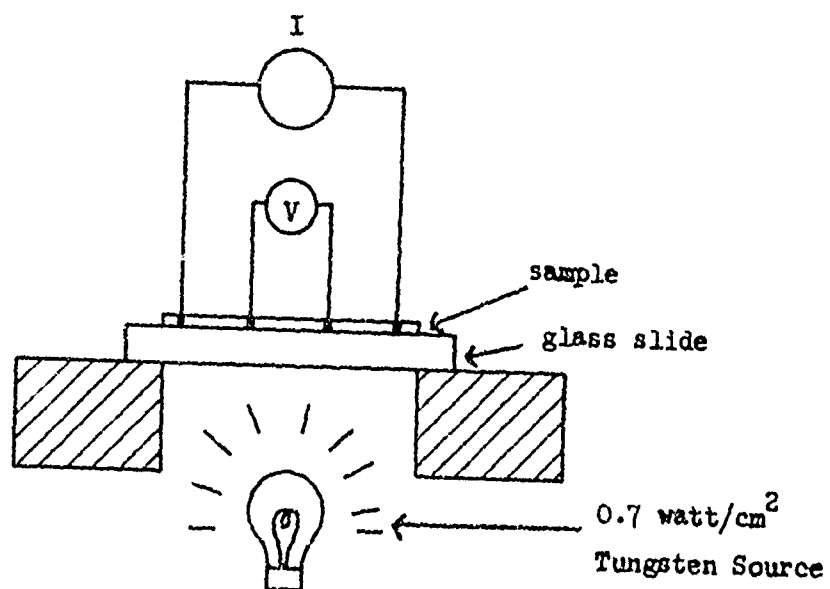


Figure 13. Apparatus Used to Test Effect of Silicon Dioxide Deposition on Lifetime

TABLE XI

Effect of Silicon Dioxide Deposition on Excess Carrier Concentration

Sample #	Description	Relative Excess Carrier Concentration (n/n _i)
1	No silicon dioxide on either side	110
2	Silicon dioxide on one side; side without silicon dioxide was illuminated	37
2	Silicon dioxide on one side; side with silicon dioxide was illuminated	46
3	Silicon dioxide on both sides	40

Transparent but electrically conducting films of aluminum were deposited on both sides of the substrate. The aluminum films were electrically isolated from the gold contacts and the germanium substrate.

The conductivity of the samples was measured with the apparatus shown in Figure 13, but with two modifications: (1) The 0.7 watt cm^2 tungsten source was replaced with a low intensity source in order to prevent heating the substrate. (2) A D.C. bias was applied to the transparent aluminum plates with respect to one of the voltage contacts.

The results of the measurements are shown in Table XII.

TABLE XII
Relative Conductivity as a Function of Surface Bias

Bias (volts)	Relative excess carrier concentration $(\frac{n}{n_i})$
10	0.11
5	0.15
0	0.22
-5	0.24
-15	0.40
-30	0.49
-41	0.72

The change in conductivity resulting from the surface charge layer induced by the bias was appropriately compensated for. The following observations can be made: (1) The rate of recombination on the surface is greater than the rate of recombination in the bulk. The excess carrier concentration at -41 volts is more than three times as great as that at 0 volts. (2) Contrary to theoretical predictions the excess carrier concentration for accumulated n-type surfaces (positive bias) does not increase with increasing bias. Furthermore the excess carrier concentration for accumulated p-type surfaces (negative bias) does not increase with increasing bias as fast as it should. Both of these effects are probably due to the drift of ions in the unannealed silicon dioxide film.

4. Conclusions

The following conclusions can be drawn from the tests which were carried out to investigate the deficiencies of the devices. (1) For devices whose open circuit output voltage is well below 0.20 volts*, the dominant deficiency is faulty contacts. (2) For devices whose open circuit voltage is nearly equal to 0.20 volts*, the dominant deficiency is excessive surface recombinations. If bulk recombination was the dominant recombination mechanism, the measurements summarized in Table XII would have been independent of bias voltage. These conclusions can be collaborated with a mathematical expression which may be used to roughly approximate the excess carrier concentration at the junctions of a p-i-n thermophotovoltaic cell in terms of the open circuit voltage:

$$\frac{n}{n_i} = \exp \frac{eV}{2kT}$$

For $V = 0.20$ volts and $T = 300^{\circ}\text{K}$, $n/n_i = 47$. This compares reasonably well with the values of 46 and 40 obtained with devices 2 and 3 in Table XI.

* This value of open circuit voltage is for samples illuminated with the 0.7 watt cm^{-2} source with the same test fixture used to obtain the results in Tables IX, X, and XI.

III. CONCLUSIONS AND RECOMMENDATIONS

As we have pointed out in our description of the experimental results, the performance of the devices which were fabricated falls far short of the performance which was predicted for devices with optimum physical parameters. The primary reasons for this are:

1. High surface recombination velocity
2. High bulk recombination
3. Poor junctions

Any future program which is directed toward the improvement of p-i-n planar photovoltaic cells should take these points into consideration. The surface recombination can be reduced through appropriate annealing procedures after the deposition of the insulating film. The alloying problems which have been discussed can be solved either by using appropriate alloying techniques or by the use of ion implantation to form the n^+ and p^+ contacts. The problem with bulk recombination reduction during processing can be eliminated by using a fabrication procedure which keeps the maximum processing temperature below 300°C . In that case very little degradation should occur in the bulk lifetime.

A maximum conversion efficiency of 14.7% was computed for an optimized device operating with illumination from an 1873°K erbium oxide source. Nearly half the energy radiated from such a source is carried by photons whose energy is below that of the germanium band gap. The use of a reflective coating which will return these photons to the source can lead to significant improvement in the operating efficiency. Future work should

include the fabrication of cells which have such reflective coatings.

Little work has been done on the present study with regard to heat sinking of the device. It is necessary that such heat sinking be accomplished because of the very rapid degradation of the device characteristics with an increase in cell temperature. Heat sinking of a p-i-n planar cell is more difficult than for a standard p-n junction cell because of the fact that the electrical contacts are both on the same surface as the heat sink, and one must simultaneously obtain the electrical isolation and good thermal contact to the surface. Any future work should include a program to minimize the temperature drop across this interface.

If the above mentioned problems can be solved, and all indications are that they can, the result should be a thermophotovoltaic cell with relatively high conversion efficiency.

REFERENCES

1. R. J. Schwartz, "A Theoretical and Experimental Investigation of Planar PIN Thermophotovoltaic Cells", Annual Report, TR ECOM-0129-1, Contract No. DAABC7-70-C-0129, August, 1971.
2. A. Reisman, R. Rhor, "Room Temperature Chemical Polishing of Ge and Ga As", J. Elec. Chem. Soc., Vol. 111, p. 1425, 1964.
3. N. Goldsmith, W. Kern, "The Deposition of Vitreous Silicon Dioxide Films from Silane", RCA Review, p. 153, March, 1967.
4. C. W. Kim, P-I-N Thermo-photo-voltaic Diode, Ph.D. Thesis, Purdue University, 1968.
5. E. P. ErNisse, Temperature Gradients in Semiconductor Alloying Technology, Ph.D. Thesis, Purdue University, 1965.
6. W. van Rousbroek, W. Shockley, "Photon-Radiative Recombination of Electrons and Holes in Germanium", Physical Review, Vol. 94, p. 1558, June 15, 1954.

APPENDIX

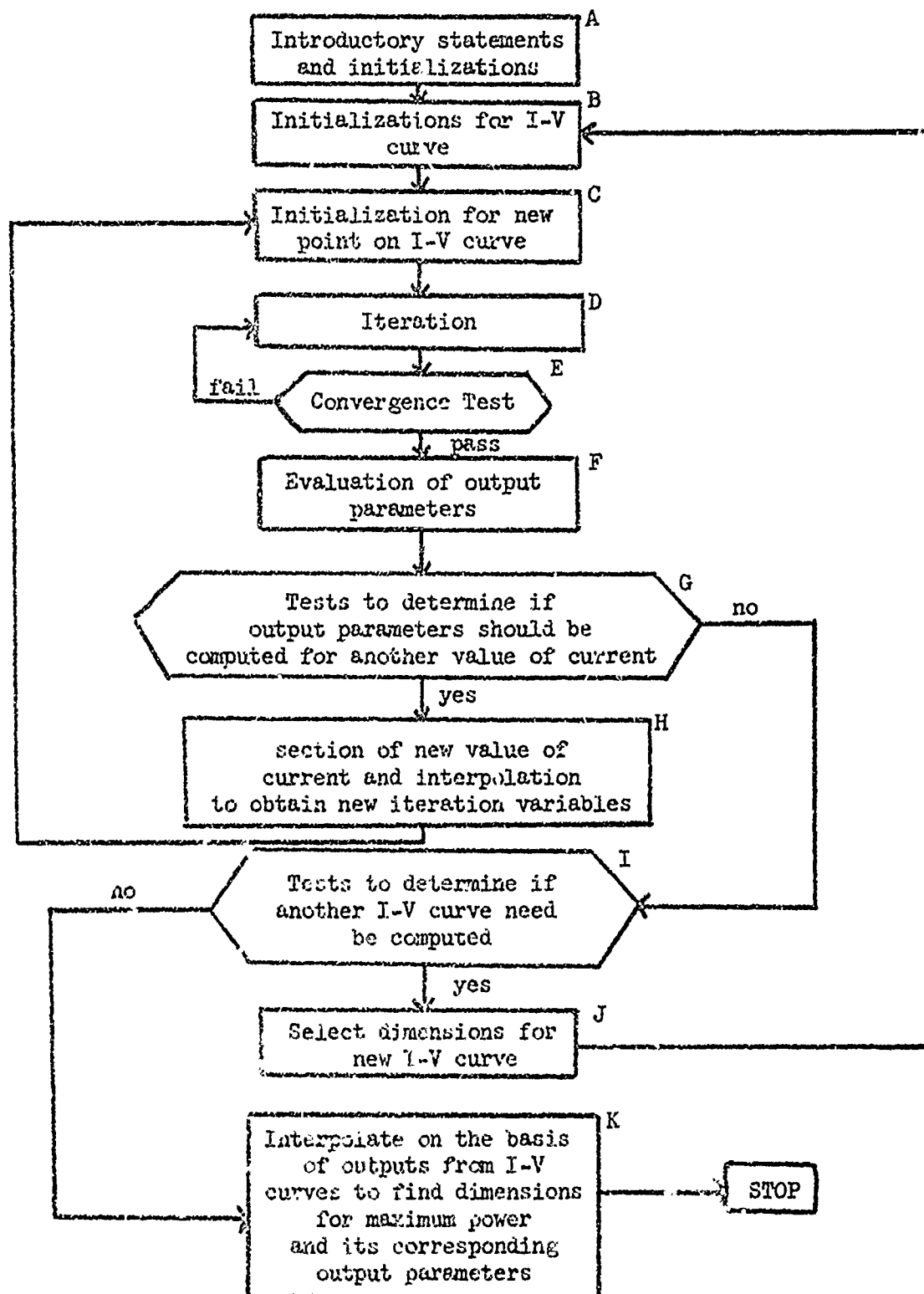
In this appendix the ADOP program will be described in some detail. The input parameters and the printed output will also be described.

Description of the Program

The program is described very briefly in the flow chart shown on page 58 . First of all the input values are set and preliminary computations and initializations are made (Box A). These input values include an initial guess of the dimensions of the device for which the maximum power will occur. The input current is initially set equal to zero (Box B). After additional initial computations done in Boxes B and C, the open circuit voltage is evaluated (Boxes D, E and F). In order to evaluate the output voltage, a boundary value problem must first be solved.* This problem is solved in the computer program by successive over-relaxation. In the successive over-relaxation process an iteration (Box D) is carried out in which a new and better estimate of the solution of the boundary value problem is obtained from an original estimate. Then a convergence test is carried out to determine if the new estimate is sufficiently close to the solution of the boundary value problem. If not, the new estimate is used in the iteration process to obtain a still better estimate. By repeated iterations and convergence tests, the estimate is successively improved until the convergence test is finally passed.

* The theoretical formulation of the boundary value problem and a detailed description of the portion of the computer program in which it is solved is included in Report No. 11.

ADOP PROGRAM



The solution of the boundary value problem is then used to compute the output voltage and other output parameters (Box F).

Once the open circuit voltage is computed, a new value of current is selected (Box H); and the computations made in Boxes C, D, E and F are repeated to obtain the output voltage for this current. This process of selecting new values of current and evaluating the corresponding values of voltage is repeated until a sufficient number of values are obtained to provide very good estimates of the short circuit current and the maximum power.

After it has been determined that the short circuit current and the maximum power can be satisfactorily estimated (Box G), a new set of dimensions is selected for the device (Box J). The process of obtaining enough points on the I-V curve to estimate the maximum power and the short circuit current is repeated for the new set of dimensions.

This process of selecting new dimensions and evaluating the output parameters for these dimensions is systematically repeated. The dimensions are selected in such a way that they tend to be close to those dimensions for which maximum power will occur.*

After it has been determined that the output parameters have been evaluated for a sufficient number of sets of dimensions (Box I), the maximum power and the dimensions for which maximum power will occur are determined by means of an interpolation process. A quadratic function of the form

$$P = A_0 + A_1 l_n + A_2 l_p + A_3 x_o + A_{11} l_n^2 + A_{22} l_p^2 + A_{33} x_o^2 + 2A_{12} l_n l_p \\ 2A_{13} l_n x_o + 2A_{23} l_p x_o$$

* The dimensions which are varied are the width of the n contact (l_n), the width of the p contact (l_p), and the thickness of the device (x_o). These dimensions must be varied in discreet increments. (See Report No. 1.)

is fitted to the values of output power associated with ten appropriately selected sets of dimensions. In the above equation P is the power output and the A's are constants. Note that since there are ten A's, ten equations (which come from the ten sets of dimensions) are needed to evaluate these A's. Once the A's are evaluated, the values of λ_n , λ_p and x_0 which maximize P are determined, and finally the maximum power is obtained.

A number of other parameters (such as open circuit voltage and short circuit current) are obtained from quadratic interpolations for the dimensions at which maximum power occurs.

Input parameters

The input parameters are listed in the three categories which are defined below: physical parameters--physical values which are needed to evaluate the performance of the device; dimension parameters--numerical values which define the dimensions of the device; program parameters--numerical values which control the speed and accuracy of the program and the amount of detail in the output.

Physical parameters

The physical parameters which are listed in statements 1650-2100 of the ADOP program are described in Table XIII. The generation rate of hole-electron pairs as a function of distance from the illuminated surface is read in at statement 4250.

TABLE XIII
LIST OF PHYSICAL PARAMETERS

FORTRAN Name	Physical Symbol(s)	Comments
KTOE	kT/e	(<u>kT over e</u>)
DP	D_p	hole diffusion coefficient
DN	D_n	electron diffusion coefficient
NI	n_i	intrinsic carrier concentration
RCOMFAC	r	<u>recombination factor</u>
VSB	$v_{S.B}$	Surface recombination velocity on <u>bottom or unilluminated surface.</u>
VST	$v_{S.T}$	surface recombination velocity on <u>top or illuminated surface</u>
VGAP	v_g	(energy gap voltage)
CURDOPT		(<u>optimum current density</u>)
		The current collected per unit area of illuminated surface if every photon capable of generating a hole-electron pair is absorbed and if every optically generated hole- electron pair is collected.

Dimension parameters

The dimension parameters which are given in statements 3100-3400
can be described concisely in the following equations:

- (1) $LN = 2 * NLNL * K$.
- (2) $LP = 2 * NLP1 * K$
- (3) $XO = NXOL * H$
- (4) $LI = NLIL * K$
- (5) $\left\{ \begin{array}{l} \text{minimum} \\ \text{value of} \\ XO \end{array} \right\} = (NXOMIN + 1) * H$

where

LN = width of n contact

LP = width of p contact

XO = thickness of device

The fortran variables $NLNL$, $NLP1$, $NXOL$, $NLIL$ and $NXOMIN$ are integers.

The variables H and K are real numbers which specify increment sizes in centimeters. (See Report No. 1.¹) The dimensions are constrained to values which are integral factors of these increments. In the ADOP program the dimensions of the device are varied by systematically varying the values of $NLNL$, $NLP1$ and $NXOL$ (Box J of the flow chart). The initial guess of the dimensions for which maximum power occurs is determined by the initially specified values of $NLNL$, $NLP1$ and $NXOL$.

In some cases the optimum thickness of a device will be much thinner than the minimum thickness attainable in practice due to limitations in technology. Therefore the program has been adapted to optimize the device under the constraint that XO will have a specified minimum attainable value. This value can be specified by appropriately choosing $NXOMIN$ and H in equation (5).

The time required to run the ADOP program can be reduced by choosing the largest possible values for H and K .¹ On the other hand, the accuracy

of results obtained increases with decreasing values of H and K.¹ Experimental runs were carried out for which the physical parameters and the device dimensions were held constant as H and K were varied. The error in the value of maximum power was made negligible by choosing sufficiently small values of H and K. The error in the value of maximum power obtained for larger values of H and K could then be estimated by comparing the maximum power obtained with larger values of H and K with that obtained with the small values of H and K. For values of H and K used to obtain the results in Tables I through VI the estimated error is 1% or less.

Program parameters

A discussion of program parameters is of little value unless one wishes to use the program. In this case a detailed description of the program will be needed. A document providing such a description will be prepared at a later date.

Printed output

Table XIV lists and describes the FORTRAN variables that appear in the printed output in the order in which they appear.

The printout can be divided into two parts. The first part gives the output for a given set of dimensions. (See Table XV) This part will be repeated for each set of dimensions for which the points on an I-V plot are to be obtained. The second part summarizes the outputs which are computed for each set of dimensions and gives information which will describe the output of the optimized device. (See Table XVI)

Output for a given set of dimensions.... The values of CURDNET, VOLTAGE and ETA for the points on the I-V curve are listed in part [B]

TABLE XIV
List of Output Parameters

Fortran variable	Description
ILE	(<u>index of linear equations</u>) A subroutine is used which solves a simultaneous system of linear equations. If ILE=0, the system is solved satisfactorily. Otherwise the system is singular to the accuracy of the computer.
PTKNT	(<u>point count</u>) an index which is chronologically associated with a point on the I-V plot.
CURDNET	(<u>current density net</u>) net current output per unit area of illuminated surface.
VOLTAGE	voltage output which is associated with a given value of CURDNET.
ETA	cell efficiency associated with a given pair of values of VOLTAGE and CURDNET. i.e. $\text{ETA} = \text{CURDNET} * \text{VOLTAGE}/\text{CURDMAX}/\text{VGAP}$.
VOC	(<u>open circuit voltage</u>)
VF	(<u>voltage factor</u>) i.e. $\text{VF} = \text{VOC}/\text{VGAP}$.
CURDSC	(<u>short circuit current density</u>) The short circuit current produced per unit area of illuminated surface.
ETACOL	(collection efficiency) i.e. $\text{ETACOL} = \text{CURDSC}/\text{CURDMAX}$.
PMAXPOW	(<u>maximum power point power</u>)

PMAXPOW	(<u>maximum power point current</u>) The current per unit area of illuminated surface at the maximum power point.
VMAXPOW	(<u>maximum power point voltage</u>)
CF	(<u>curve factor</u>) i.e. $CF = PMAXPOW/VOC / CURDSC$.
ETACELL	(<u>cell efficiency</u>) i.e. $ETACELL = PMAXPOW / POWMAX$.
XO	the thickness of the photovoltaic cell.
LN	width of the n contact
LP	width of the p contact
LI	spacing between contacts.
H }	increment sizes
CURDOPT	optimum current density; the current collected per unit area of illuminated surface if every photon capable of generating a hole-electron pair is absorbed and if every optically generated hole-electron-pair is collected.
ISE	(<u>index of symmetrical equations</u>) A subroutine is used which solves the simultaneous system of equations whose coefficient matrix must be positive definite or negative. If ISE=0, the system is solved satisfactorily. Otherwise the coefficient matrix is either singular to computer accuracy or is not positive or negative definite.

ID	(index of dimensions) an index which is chronologically associated with a set of dimensions for which the points for an I-V plot are obtained.
ETAC	same as ETACOL
ETACE	same as ETACELL
CURDMAX	(maximum current density) the current output per unit area of illuminated cell when all generated hole-electron pairs are collected.
POWMAX	(maximum attainable power) the power output per unit area of illuminated surface when all the generated hole-electron pairs are collected with an output voltage equal to the energy gap voltage. I.e. POWMAX= CURDMAX * VGAP.
ETAABS	(CURDMAX/CURDOPT) the ratio of the number of carriers generated in the finite thickness device to the number of carriers generated in an infinitely thick device.

TABLE XV

Printed Output for a Given Set of Dimensions

[D]	[E]	[F]	
43	1.318E+17	1.318E+17	
44	1.164E+17	1.162E+17	
21	9.904E+16	9.873E+16	
20	7.869E+16	7.823E+16	
25	5.249E+16	5.187E+16	
34	1.714E+16	1.640E+16	
51	5.758E+15	4.981E+15	
ILE = 0			
45	3.340E+16	3.270E+16	
ILE = 0			
ILE = 0			
54	2.480E+15	1.690E+15	
21	1.379E+15	5.823E+14	
30	1.001E+15	2.023E+14	
20	8.708E+14	7.079E+13	
20	8.251E+14	2.473E+13	

PTKNT	CURDNET	VOLTAGE	ETA	
1	0.	4.439E-01	0.	
2	8.089E-01	4.372E-01	1.325E-01	
3	1.618E+00	4.284E-01	2.596E-01	
4	2.427E+00	4.159E-01	3.780E-01	
5	3.236E+00	3.935E-01	4.770E-01	
6	3.892E+00	3.286E-01	4.791E-01	
7	3.992E+00	2.548E-01	3.811E-01	
8	3.654E+00	3.680E-01	5.038E-01	
9	4.011E+00	1.830E-01	2.750E-01	
10	4.016E+00	1.171E-01	.762E-01	
11	4.017E+00	6.494E-02	9.774E-02	
12	4.018E+00	2.676E-02	4.028E-02	
13	4.018E+00	8.595E-04	1.294E-03	

VOC	=	.4439	
VF	=	.6726	
CURDSC	=	4.018E+00	
ETACOL	=	.9935	
PMAXPOW	=	1.345E+00	
CMAXPOW	=	3.664E+00	
VMAXPOW	=	.3670	
CF	=	.7539	
ETACELL	=	.5038	
XO	=	5.000E-02	
LN	=	1.500E-02	
LP	=	2.500E-02	
LI	=	2.500E-03	

TABLE XVI
Summary of Outputs for Given Sets of Dimensions and Output for Optimized Device

H = 1.000E-02 K = 2.500E-03 L1 = 2.500E-03 CURDOPT = 5.000E-00 ISE = 0									
ID	LN	LP	XO	VOC	VF	CURDSC	ETAC	CURIMAX	CHAXPOW
1	3	4	.4494	.6809	3.934E+00	.9964	3.948E+00	3.611E+00	.3738
2	2	4	.4494	.6809	3.935E+00	.9967	3.948E+00	3.610E+00	.3738
3	4	4	.4494	.6809	3.933E+00	.9960	3.948E+00	3.609E+00	.3737
4	3	3	.4494	.6809	3.933E+00	.9960	3.948E+00	3.610E+00	.3738
5	3	5	.4494	.6809	3.935E+00	.9967	3.948E+00	3.611E+00	.3738
6	3	4	.4563	.6913	3.815E+00	.9985	3.820E+00	3.522E+00	.3818
7	3	4	.4539	.6726	4.016E+00	.9931	4.044E+00	3.664E+00	.3671
8	2	5	.4494	.6809	3.933E+00	.9966	3.948E+00	3.609E+00	.3737
9	2	4	.4439	.6726	4.018E+00	.9935	4.044E+00	3.564E+00	.3671
10	3	5	.4439	.6726	4.018E+00	.9935	4.044E+00	3.664E+00	.3670

H = 1.000E-02 K = 2.500E-03 L1 = 2.500E-03 CURDOPT = 5.000E-00 ISE = 0	LN	= 1.285E-02
	LP	= 1.968E-02
	XO	= 4.012E-02
	VOC	= .4493
	VF	= .6808
	CURDSC	= 3.936E+00
	ETACOL	= .9965
	CURIMAX	= 3.950E+00
	CHAXPOW	= 3.612E+00
	WMAXPOW	= .3738
	PMAXPOW	= 1.350E+00
	POUTMAX	= 2.607E+00
	CF	= .7634

-68-

[D]

[E]

or Table XV. The column labeled PTXINT lists indices which are chronologically assigned to each set of values CURDNET, VOLTAGE and ETA.

In part [A] the reader will note that there are ten rows of numbers excluding the rows containing the expression, ILE = 0. Each of these rows corresponds to a row in part [B] with the first row in [A] corresponding to the first row in [B], the second row in [A] with the second row in [B], etc. The column designated by [D] gives the number of iterations required for convergence. The column designated by [E] gives the excess carrier concentrations in the middle of the n contact. The column designated by [F] gives the excess carrier concentration in the middle of the p contact.

The expressions ILE = 0 result from a curve fitting routine which is used to estimate the value of CURDNET for which the maximum power will occur. (See Table XIV. .)

In part [C] the output parameters and dimensions of the cell are listed.

Summary of outputs for each set of dimensions and output of optimized device.-- The cell dimensions for which output parameters have been computed and the corresponding output parameters are summarized in part [D] of Table XV. The columns headed by LN and LP list half the number of increments on the n and p contacts, and the column headed by XO lists the number of increments along the dimension of the device that is perpendicular to the illuminated surface. (The values listed under LN, LP and XO are equal to the values NLN1, NLP1 and NXO1 ascribed on page 62). Note that the row of values corresponding to the number 9 in the column headed by LD is obtained from Table XV.

The list of values in part [E] of Table XVI gives the dimensions and output parameters of the optimally designed device.

The array of points shown in part [B] of Table XVI may be represented algebraically by the array shown below:

λ_1	λ_2	λ_3
v_{1in}	v_{1ip}	v_{1xo}
v_{2in}	v_{2ip}	v_{2xo}
v_{3in}	v_{3ip}	v_{3xo}

This array consists of the eigenvalues and orthonormal eigenvectors of the symmetric matrix with elements A_{ij} . The power may be expressed in the equation:

$$P = P_{MAXPOW} + \lambda_1 v_1^2 + \lambda_2 v_2^2 + \lambda_3 v_3^2$$

$$\text{where } v_i = v_{iin} (n_{in} - \bar{n}_{in}) + v_{iip} (n_{ip} - \bar{n}_{ip}) + v_{ixo} (n_{xo} - \bar{n}_{xo})$$

for $i = 1, 2$ and 3 .

Preceding page blank

PROGRAM MAIN (INPUT,OUTPUT,TAPE5=INPUT,TAPE6=OUTPUT)

```

REAL LN,LPI,LI,NSINITE,NO,K,M,MDPEOK,MAGIDUM,MAGIMAX,NT,NOPPO,NSMAX
I,KTOE,AN,NP,JUNCOT,LNJOMJ,NST2,NO2,VS4,NO4,KO2DNEH,KO2DPEH,EL(200
21,W(200),X(200),Y(200),Z(200),CRNT(100),VOLT(100),NS1(22,49),NS2(2
32,49),NS3(22,49),MAGI1(22,49),MAGI2(22,49),MAGI3(22,49),NS(22,49),
4MAGI(22,49),DJMMY(22,49),DUMAG(22,49),DNNT(22,49),NEI(22,49),CURDX
5(49),CURDY(49)
REAL NSBAR,NSSBAR,NT2,GBULK(22)
REAL NCINC,N1,N2,N3,NSRF
INTEGER R,S,RH,SH,RP1,SP1,RHP1,SHP1
INTEGER RH2
INTEGER RI,RIM1,SIP1,SI
INTEGER PATHKNT,PATHNMB
INTEGER PTKNT
REAL NLN,NLP,NXO,NL1,VOC0(50),VFD(50),CURDSRD(50),ETACOLD(50),
1PMXPOND(50),CMXPOND(50),V4XPOND(50),CFO(50),ETAD(50),CURDMXD(50)
DIMENSION XM(3,1),EIGVAL(3)
DIMENSION CUMGEV(82)
COMMON IET,JLNP,JLNH,JLPP,JLPM,JXDP,JXOM,LNLP,LNXO,LPXO,RICLN,
1RICLP,RICXO,BM(3,1),AM(3,3),JVLNT(50),JVLPI(50),JNXO(50),ID

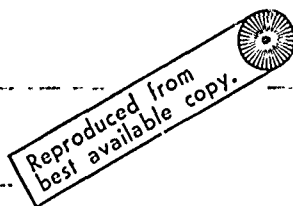
```

LISTING OF PHYSICAL PARAMETERS

```

KTDE=0.0259
UP=48.0
DN=96.0
NI=2.5E13
PD=NI
RCOMPAC=2.8E-14
VSB=100.
VST=100.
VGAP=0.65
CURDOPT=1.

```



LISTING OF PROGRAM PARAMETERS

```

IC=2
NESHNMN=1
IH=2
LL=0
IMAX=150
LCOPMIN=20
ITVAR=1
IPATH=1
ICURVP=0
EPSILON=0.001
NCINC=5.0
RF=0.35
FACTDR=5.0

```

LISTING OF DIMENSION PARAMETERS

```

NAT=NI=6
DT=0.1-10
LI=LXCI=4
NS=2
NL=NL1=1
.125E-2*12.
0.25E-2

```

LISTING OF RELAXATION FACTORS

OMEGAB=1.92	3450
OMEGAS=1.4	3500
OMEGABH = 1.92	3550
OMEGASB=0.9	3600
OMEGAST=1.4	3650
OMEGAC=1.4	3700
OMEGACH=1.4	3750

EVALUATION OF SCALE FACTOR AND READIN AND SCALING OF CUMGEN

READ(5,685) CJRDSCL	4000
SCALE=CURDOPT/CJRDSCL	4050
DO 3 NX=1,82	4100
READ(5,685) CJMGEN(NX)	4150
CUMGEN(NX)=CJMGEN(NX)*SCALE	4200
GSURF=CUMGEN(1)-CUMGEN(1)	4250

LISTING OF FIXED CONSTANTS AND PRELIMINARY COMPUTATIONS

U=LMAX-LH	4450
ALPHA=2.0*CN*DP/(DN+DP)	4500
NC=NI+NI/PC	4550
NOPPO=NC+PO	4600
OPNO=PO+NO	4650
NC2=PO2+POPO	4700
PO2=PO+PO	4750
PO4=PO2+PO2	4800
NC2=NO+NO	4850
NO2=NO2+NO2	4900
ECC=(PC+NC)/2.	4950
LC=DP*PO+DN*NO)/(DP+DN)	5000
NL=NI+NI	5050
D=0	5100
I=IC	5150
OPTS=0	5200
DXXOM=3	5250



BEGIN LOOP FOR EVALUATION OF POINTS ON I-V CURVE

D=ID+1	5400
LN=NLN1	5450
NLP=NLP1	5500
YD=NX01	5550
INITL=NLN1+NLP1+NL1	5600
INITL=NX01	5650
H=LN*K*2.0	5700
F=NLP*K*2.0	5750
=NL1-K	5800
LNK0*XH	5850
BRUNET=0.0	5900
AB=H/12.5E-4+0.5	5950
IGEN=CUMGEN(NY01*N(H+2))-CUMGEN(2)	6000
AN=1	6050
ANKE,A=1	6100
URDMAX=(GSURF+BULKGEN)*1.6E-19	6150
VDMAX=CURDMAX*VG/P	6200
ID=(LPL+1)/2.0+1	6250
UDS=4EHA*EPSILON*(XDXOM*YD)	6300

C LISTING OF TERMS THAT MUST BE RESET FOR NEW VALUES OF CURDNET 151
C 10 I=INITL 77
C J=JINITL 78
C MESHKNT=1 79
C
C VALUE OF INDXITL SET TO CAUSE INITIALIZATION 80
C
C INDXITL=0 81
C
C EVALUATE I AND J DEPENDENT TERMS 83
C
C COMPUTATION OF INCREMENT SIZES 85
C
C 30 REALI=I 87
C H=XO/REALI 89
C REALJ=J 90
C K=((LN+LP)/2.+LI)/REALJ 91
C
C COMPUTATION OF INCREMENT DEPENDENT VARIABLES 92
C
C AK=ALPHA/(K*K) 93
C AH=ALPHA/(H*H) 94
C H02DNE=H/2.0/DN/1.6E-19 95
C H02DPE=H/2.0/DP/1.6E-19 96
C MDPFOK=-DP*1.6E-19/K 97
C H2=2.0*H 98
C DNEOK=DN*1.6E-19/K 99
C AH2PAK2=2.0*AH+2.0*AK 100
C P2=2.0*RCOMFAC 101
C HSOKS=H*H/K/K 102
C HSOKSP1=HSOKS+1.0 103
C HOATGS=H/ALPHA*GSURF 104
C DP2EKOH=DP*2.0*1.60E-19*K/H 105
C DN2EKOH=DN*2.0*1.6E-19*K/H 106
C KO2DNEH=K/2.0/DN/1.6E-19/H 107
C KO2DPEH=K/2.0/DP/1.6E-19/H 108
C H02DNEK=H/2.0/DN/1.6E-19/K 109
C HC2DPEK=H/2.0/DP/1.6E-19/K 110
C HVST02A=H*VST/2.0/ALPHA 111
C HVSB02A=H*VS02/2.0/ALPHA 112
C
C LISTING OF ITERATION INDICES 113
C
C RH=LN/(2.*K)+0.5 114
C SH=(LN/2.+LI)/K+1.5 115
C S=SH 116
C RHP1=RH+1 117
C R=RHP1 118
C SHP1=SH+1 119
C RPI=R+1 120
C SP1=S+1 121
C JH=J+1 122
C JN=J+2 123
C IH=I+2 124
C IN=IH 125
C JHMI=IH-1 126
C JNMI=JN-1 127
C INMI=IN-1 128
C IHMI=IH-1 129

LISTING OF TERMS DEPENDENT ON ITERATION INDICES

SMR=S-R
RJNM2=JN-2
TERM1=N1+(VST+VS8*SMR/RJNM2)/R2/X0
TERM2=VST/R2/X0/RJNM2
TERM3=VS8/R2/X0/RJNM2
BULKPTS=(IN-2)*(JN-2)

EVALUATION OF GBULK

ICJ=I*NIH+2
DO 35 NX=2, INH1
ICL=ICJ-NIH
GBULK(NX)=(CJMGEN(ICJ)-CJMGEN(ICL))/H
ICJ=ICL

LISTING OF TESTPOINT INDICES

INDXXC=(IN+2)/2
INDXYC=(JN+2)/2
INDXXF=IN-1
INDXNN=R
INDXPN=SP1



LISTING OF TERMS THAT MUST CHANGE WITH EACH NEW VALUE OF CURSONT

GBADXR=(GSJRF+GBULKGEN-CURDNET/1.6F-19)/X0/RCOMFAC
NSINITL=-1 ERHRSURE(TERM1*TERM1+GBADXR)

INITIALIZATION OF MAGI AND VS

IF(INDXILL.NE.0) GO TO 45
INDEXILL=1
IP2=I+2
JP2=J+2
DO 20 NX=1,IP2
DO 20 NY=1,JP2
MAGI(NX,NY)=0.0
20 NS(NX,NY)=NSINITL
NSMAX=FACTOR*(1+VS*SQRT(N1*(1+GBADXR)))

BOUNDARY CONDITIONS ON MAGI ON THE BACK SURFACE OF THE CAVITIES

40 MAGIMAX=CIRMM1*((L2D1*V1/2.08L1))
DO 50 NY=RPH1,SP1
50 MAGI(2,NY)=MAGIMAX
DELTAL=CIRMM1*V1/2*PAK2+R2*(VSMAX*FACT)
DELTALC=CIRMM1*V1*ESAF*DELFACT

RESET LCOOKNT = 0

LCOOKNT=0

PRINT 17, 'ITERATION NUMBER'

60 IF(LCOOKNT.GE.1000) THEN 70, 1000, 1000
1000 PRINT 17, 'ITERATION NUMBER'
1000 ENDIF
60 DO 70 NK=1,1000

10 WRITE (6,550) (NS(NX,NY),NY=1,JN)
11 WRITE (6,560)
12 DO 80 NX=2,IH
13 80 WRITE (6,550) (MAGI(NX,NY),NY=1,JH)
14 WRITE (6,560)
15 IF((LOOPKNT.GE.LMAX).AND.(IDXETA.EQ.1)) GO TO 228
16 IF(LOOPKNT.GE.LMAX) GO TO 515
17 LOOPKNT=LCOPKNT+1
18 C
19 C P CONTACT--APPROXIMATION OF MAGI AND VS, AND EVALUATION OF W AND Y
20 C
21 IF(SP1.EQ.JNM1) NS(1,SP1)=VS(2,SP1)
22 1+HO2DPEK*(MAGI(2,SHP1)-MAGI(2,SH))
23 IF(SP1.EQ.JNM1) GO TO 115
24 W(SH)=0.0
25 Y(SP1)=1.0
26 DO 100 NY=SHP1,JHM1
27 NST2=NS(2,NY)+NS(1,NY)
28 GP=DP2EKOH*(NST2+POPNO)/(NST2+VD2)
29 NS4=NS(2,NY+1)+NS(2,NY)+VS(1,NY+1)+VS(1,NY)
30 GN=K02DNEH*(NS4+P04)/(NS4+P02PV02)
31 MAGI(2,NY)=MAGI(2,NY-1)-GP*(VS(2,NY)-VS(1,NY))
32 W(NY)=W(NY-1)+GP*Y(NY)
33 NS(1,NY+1)=NS(1,NY)-GN*(3.0*(MAGI(3,NY)-MAGI(2,NY))-(MAGI(4,NY)-MA
34 GI(3,NY)))-(NS(2,NY+1)-NS(2,NY))
35 100 Y(NY+1)=Y(NY)+(GN+GN+GN)*W(NY)
36 C
37 C P CONTACT--EVALUATION OF DELTA
38 C
39 NST2=NS(2,JNM1)+NS(1,JNM1)
40 GP=DP2EKOH*(NST2+POPNO)/(NST2+VD2)
41 DELTA=(MAGI(2,JH)-MAGI(2,JHM1)+GP*(NS(2,JNM1)-NS(1,JNM1)))/(R(JHM1
42 1)+GP*Y(JNM1))
43 C
44 C P CONTACT--EVALUATION OF MAGI AND VS
45 C
46 DO 110 NY=SHP1,JHM1
47 MAGI(2,NY)=MAGI(2,NY)+W(NY)*DELTA
48 110 NS(1,NY)=NS(1,NY)+Y(NY)*DELTA
49 NS(1,JNM1)=NS(1,JNM1)+Y(JNM1)*DELTA
50 C
51 C NCCONTACT--APPROXIMATION OF MAGI AND VS, AND EVALUATION OF W AND Y
52 C
53 115 IF(R.EQ.2) NS(1,2)=NS(2,2)-0.2DNEK*(MAGI(2,2)-MAGI(1,2))
54 IF(R.EQ.2) GO TO 135
55 W(1)=0.0
56 Y(2)=1.0
57 DO 120 NY=2,RH
58 NST2=NS(2,NY)+NS(1,NY)
59 GN=DNEKOH*(NST2+POPNO)/(NST2+VD2)
60 NS4=NS(2,NY+1)+NS(2,NY)+VS(1,NY+1)+VS(1,NY)
61 GP=K02DNEH*(NS4+P04)/(NS4+P02PV02)
62 MAGI(2,NY)=MAGI(2,NY-1)+GN*(VS(2,NY)-VS(1,NY))
63 W(NY)=W(NY-1)+GN*Y(NY)
64 NS(1,NY+1)=NS(1,NY)+P04*(MAGI(3,NY)-MAGI(2,NY))-(MAGI(4,NY)-M
65 AGI(3,NY))-(NS(2,NY+1)-NS(2,NY))
66 120 Y(NY+1)=Y(NY)+(GN+GN+GN)*W(NY)
67 C
68 C P CONTACT--EVALUATION OF DELTA
69 C
70 NST2=R(2)+NS(1,R)



```

CN=DN2EKOH*(NST2+POPNO)/(NST2+PO2)
DELTA=(MAGI(2,RHP1)-MAGI(2,RH)-GN*(VS(2,R)-VS(1,R)))/(W(RH)-GN*Y(R))
111

N CONTACT--EVALUATION OF MAGI AND VS

DO 130 NY=2,RH
MAGI(2,NY)=MAGI(2,NY)+W(NY)*DELTA
130 NS(1,NY)=NS(1,NY)+Y(NY)*DELTA
NS(1,R)=NS(1,R)+Y(R)*DELTA

NS IN INTERIOR REGION

5 DELTAT=DELTATC
DO 150 NX=2,INM1
DC 140 NY=2,JNM1
DNDT(NX,NY)=AH*(VS(NX+1,NY)-VS(NX,NY)-NS(NX,NY)+NS(NY-1,NY))+AK*(A
1S(NX,NY+1)-NS(NX,NY)-NS(NX,NY)+VS(NX,NY-1))+GBULK(NX)-RCDPFAC*AS(N
2X,NY)*(NS(NX,NY)+NOPPO)
NS(NX,NY)=NS(NX,NY)+DNDT(NX,NY)*DELTAT
IF (NS(NX,NY).LT.1.0) VS(NX,NY)=1.0
140 IF (NS(NX,NY).GE.NSMAX) VS(NX,NY)=NSMAX
150 DELTAT=DELTATB

EVALUATION OF NEI

DO 160 NX=2,INM1
DO 160 NY=2,JNM1
160 NFI(NX,NY)=1.0/(NS(NX,NY)+ACCC)

MAGI IN INTERIOR REGION

CMEGAH=CMEGACH
DC 170 NX=3,IHM1
NXPL=NX+1
NXM1=NX-1
DO 170 NY=2,JHM1
NYP1=NY+1
MAGIDJM=((NFI(NX,NYP1)+NEI(NX,NY))*MAGI(NXPL,NY)+(NEI(NXM1,NYP1)+N
1EI(NXM1,NY))*MAGI(NYM1,NY)+H17KS*((NEI(NX,NYP1)+NEI(NXM1,NYP1))/RA
2GI(NX,NYP1)+(NEI(NX,NY)+NEI(NXM1,NY))*MAGI(NX,NY-1))/(HSOKSP1*(A
3I(NX,NYP1)+NEI(NXM1,NYP1)+NEI(NX,NY)+NEI(NXM1,NY)))
MAGI(NX,NY)=MAGI(NX,NY)*CMEGAH*(G1G2H-M1-M2)/(X1*X2)
171 CMEGAH=CPLGABH

NS AT TOP SURFACE

DO 180 NY=2,JNM1
M=NS(INM1,NY)+H17ATGS-HVSTD2AA(NS(INM1,NY)+VS1(NY))
180 NS(IN,NY)=NS(IN,NY)*CMEGAST/M-NS(IN,NY))

NS AT BOTTOM SURFACE

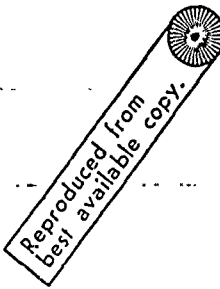
IF (RP1.GE.S) GO TO 200
DO 190 NY=2,JNM1
M=NS(IN,NY)+H17ATGS-HVSTD2AA(NS(IN,NY)+VS1(NY))
190 NS(IN,NY)=NS(IN,NY)*CMEGAST/M-NS(IN,NY))

NS AT LEFT SIDE

DO 210 NX=1,INM1

```

M=NS(NX,2)
 /10 NS(NX,1)=NS(NX,1)+OMEGAS*(M-VS(NX,1))
 NS AT RIGHT EDGE
 DO 220 NX=1,IN
 M=NS(NX,JNM1)
 NS(NX,JN)=NS(NX,JN)+OMEGAS*(M-VS(NX,JN))
 EVALUATION OF DELTANS AND RESET OF VALUE OF NS
 SUM=0.0
 SUMS=0.0
 DO 222 NX=2,INM1
 DO 222 NY=2,JNM1
 SUM=SJM+NS(NX,NY)
 222 SUMS=SUMS+NS(NX,NY)*NS(NX,NY)
 NSBAR=SUM/BJLKPTS
 NSSBAR=SJM/BJLKPTS
 SIGMANT=0.0
 DO 223 NY=2,JNM1
 SIGMANV=SIGMANT+NS(1,NY)+VS(1,NM1,NY)
 SIGMANE=0.0
 IF(RP1.GT.S) GO TO 225
 DO 224 NY=RP1,S
 SIGMANB=SIGMANB+NS(2,NY)+VS(1,NY)
 B02=NSBAR+TERM1
 C=NSSBAR+NI2*NSBAR+TERM2*SIGMANT+TERM3*SIGHANB-GBAOXOR
 IF((B02*B02).LT.C) GO TO 515
 DELTANS = - B02 + SQRT(B02*B02 - C)
 DO 225 NX = 1,IN
 DO 225 NY = 1, JN
 NS(NX,NY)=NS(NX,NY)+DELTANS
 ENSURE THAT ENOUGH ITERATIONS HAVE TAKEN PLACE FOR STABILIZATION
 IF (LOOPKNT.LT LOOPMIN) GO TO 60
 CONVERGENCE TEST
 AEDOONS=AEDOONS*NSINITL
 IF(AEDOONS.LT.ABS(CNDT(2,INDXXN))) GO TO 60
 IF(AEDOONS.LT.ABS(CNDT(2,INDXPN))) GO TO 60
 IF(AEDOONS.LT.ABS(CNDT(INDXXXF,INDXYC))) GO TO 60
 IF(AEDOONS.LT.ABS(CNDT(INDXXG,INDXYC))) GO TO 60
 WRITEOUT FOR SUCCESSFUL EXIT
 IF(LITVAR.EQ.1) GO TO 250
 WRITE(6,540)
 WRITE(6,570) MESHKNT,LOOPKNT
 WRITE(6,450)
 DO 230 NX=1,IN
 WRITE(6,550) NS(NX,NY),NY=1,JN
 WRITE(6,560)
 C 241 NX=2,IN
 WRITE(6,561) NS(NX,NY),NY=1,JN
 WRITE(6,562)
 EVALUATION OF TERMS RELATED TO OUTPUT VOLTAGE AND POWER



50 PATHNMB=R-I	34100
KN=R	34200
KP=SP1	34300
KX=2	34400
DO 310 PATHKNT=1,PATHNMB	34500
EVALUATION OF EXCESS CARRIER CONCENTRATIONS AT JUNCTIONS	34600
NN=(NS(2,KN)+NS(1,KN))/2.0	34700
NP=(NS(2,KP)+NS(1,KP))/2.0	34800
IF(I PATH, EQ.1) GO TO 255	34900
WRITE(6,580) MESHKNT,PATHKNT	35000
WRITE(6,550) NN, NP	35050
CONTINUE	35100
IF(KN.EQ.2) WRITE(6,610) LDOPKNT,NV,NP	35200
IF ((NN.GT.0.0).AND.(NP.GT.0.0)) GOTO 260	35230
IF ((MESHKNT.EQ.MESHNMB).AND.(KN.EQ.2)) GO TO 515	35260
GO TO 300	35300
INITIAL POINTS IN THE GRAPHICAL INTEGRAL ALONG THE X AXIS	35400
35500	35500
35600	35600
260 PTNE=(NN+NS(2,KN))/2.0+ACCC	35700
PTDHDY=(3.0*(MAGI(2,KN)-MAGI(2,KN-1))/K+(MAGI(3,KN)-MAGI(3,KN-1))/	35800
1K)/4.0	35900
GIXN=PTDHDY/PTNE*H/2.0	36000
PTNE=(NP+NS(2,KP))/2.0+ACCC	36100
PTDHDY=(3.0*(MAGI(2,KP)-MAGI(2,KP-1))/K+(MAGI(3,KP)-MAGI(3,KP-1))/	36200
1K)/4.0	36300
GIXP=PTDHDY/PTNE*H/2.0	36400
EVALUATION OF GRAPHICAL INTEGRALS ALONG THE X AXIS	36500
36600	36600
36700	36700
36800	36800
36900	36900
IF (KX.LT.3) GO TO 280	37000
DO 270 NX=3,KX	37100
PTNE=(NS(NX-1,KN)+NS(NX,KN))/2.0+ACCC	37200
PTDHDY=(MAGI(NX,KN)-MAGI(NX,(N-1))/K	37300
GIXN=GIXN+PTDHDY/PTNE*H	37400
PTNE=(NS(NX-1,KP)+NS(NX,KP))/2.0+ACCC	37500
PTDHDY=(MAGI(NX,KP)-MAGI(NX,(P-1))/K	37600
270 GIXP=GIXP+PTDHDY/PTNE*H	37700
EVALUATION OF GRAPHICAL INTEGRAL ALONG THE Y AXIS	37800
37900	37900
38000	38000
280 KPM1=KP-1	38100
GIY=0.0	38200
DO 290 NY=KN,KPM1	38300
PTNE=(NS(KX,NY)+NS(KX,NY+1))/2.0+ACCC	38400
PTDHDY=(MAGI(KX+1,NY)-MAGI(KX,NY))/H	38500
290 GIY=GIY+PTDHDY/PTNE*K	38600
EVALUATION OF OJTPJT VOLTAGE, POWER AND EFFICIENCY	38700
38800	38800
38900	38900
OHMLOSS=KTDF/1.6E-19/(DN+DP)*(GIXN-GIY-GIXP)	39000
DIFFPOT=KTDF*(DN-DP)/(DN+DP)* ALOG((NP+ACCC)/(NN+ACCC))	39100
JUNC POT=KTDF* ALOG((NV+NO)*(NP+PD)/VI/VI)	39200
VOLTAGE=JJNC POT+DIFFPOT-OHMLOSS	39300
POWER=VOLTAGE*CJRDNFT	39400
ETAP=POWER/POWMAX	39500
ETACURD=CJRDNFT/CURDMAX	39500
ETAV=VOLTAGE/VGAP	39700
	39800

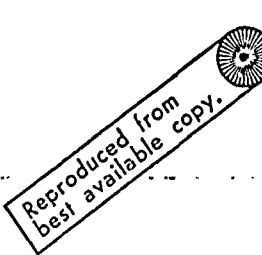
WRITEOUT OF VALUES RELATED TO CURVET, VOLTAGE AND POWER 3990
 IF (IPATH.EQ.1) GO TO 300 4000
 WRITE (6,550) CJRDNET,VOLTAGE,JUNCPOUT,DIFFPOT,OHMLOSS 4005
 WRITE (6,550) POWER,POWERMAX,ETA,ETACURD,ETAV 4010
 RESET OF PATH OF INTEGRATION 4015
 4020
 4025
 4030
 4035
 4040
 4045
 4050
 4055
 4060
 4065
 4070
 4075
 4080
 4085
 4090
 4095
 4100
 4105
 4110
 4115
 4120
 4125
 4130
 4135
 4140
 4145
 4150
 4155
 4160
 4165
 4170
 4175
 4180
 4185
 4190
 4195
 4200
 4205
 4210
 4215
 4220
 4225
 4230
 4235
 4240
 4245
 4250
 4255
 4260
 4265
 4270
 4275
 4280
 4285
 4290
 4295
 4300
 4305
 4310
 4315
 4320
 4325
 4330
 4335
 4340
 4345
 4350
 4355
 4360
 4365
 4370
 4375
 4380
 4385
 4390
 4395
 4400
 4405
 4410
 4415
 4420
 4425
 4430
 4435
 4440
 4445
 4450
 4455
 4460
 4465
 4470
 4475
 4480
 4485
 4490
 4495
 4500
 4505
 4510
 4515
 4520
 4525
 4530
 4535
 4540

START A NEW MESH UNLESS THE FINEST MESH HAS JUST BEEN COMPLETED
 IF (MESHKNT.NE.MESHNMB) GO TO 450
 BEGIN STORAGE AND INTERPOLATION WITH PROCEDURE FOR FIRST ITERATION
 IF (PTKNT.NF.1) GO TO 340
 DO 320 NX=1,IN
 DO 320 NY=1,JN
 320 NS2(NX,NY)=NS(NX,NY)
 DO 330 NX=2,IHM1
 DO 330 NY=2,JHM1
 MAG12(NX,NY)=MAGI(NX,NY)
 V2=VOLTAGE
 VOLT(1)=V2
 C2=CJRDNET
 CRNT(1)=C2
 PTKNT=2
 EVALUATION OF CURRENT AND VOLTAGE INCREMENTS
 CINCREG=CJRDMAX/NCINC
 CJRDINC=CINCREG
 CURDNET=CJRDNET+CURDINC
 GO TO 10
 INTERPOLATION PROCEDURE FOR SECOND ITERATION
 IF (PTKNT.NE.2) GO TO 390
 DO 350 NX=1,IN
 DO 350 NY=1,JN
 350 NS1(NX,NY)=NS(NX,NY)
 DO 350 NX=2,IHM1
 DO 350 NY=2,JHM1
 MAG11(NX,NY)=MAGI(NX,NY)
 V1=VOLTAGE
 VOLT(2)=V1
 C1=CJRDNET
 CRNT(2)=C1
 PTKNT=3
 CURDNET=CJRDNET+CJRDINC
 DO 370 NX=1,IN
 DO 370 NY=1,JN
 370 NS(NX,NY)=NS1(NX,NY)+NS1(NX,NY)-NS2(NX,NY)
 DO 360 NX=2,IHM1
 DO 360 NY=2,JHM1
 MAG1(NX,NY)=MAGI1(NX,NY)+MAGI1(NX,NY)-MAGI2(NX,NY)

GO TO 440	45500
BEGIN QUADRATIC INTERPOLATIONS WITH INITIALIZATIONS	45500
C3=C2	45700
C2=C1	45800
C1=CURDNET	45900
CRNT(PTKNT)=C1	46000
V3=V2	46100
V2=V1	46200
V1=VOLTAGE	46300
VOLT(PTKNT)=V1	46400
COMPUTATION OF MATRIX ELEMENTS	46500
D11=-1.0/(C3-C1)/(C1-C2)	46600
D12=-1.0/(C1-C2)/(C2-C3)	46700
D13=-1.0/(C2-C3)/(C3-C1)	46800
D21=(C2+C3)/(C3-C1)/(C1-C2)	46900
D22=(C3+C1)/(C1-C2)/(C2-C3)	47000
D23=(C1+C2)/(C2-C3)/(C3-C1)	47100
D31=-C2*C3/(C3-C1)/(C1-C2)	47200
D32=-C3*C1/(C1-C2)/(C2-C3)	47300
D33=-C1*C2/(C2-C3)/(C3-C1)	47400
EVALUATION OF VOLTAGE COEFFICIENTS	47500
A1=011*V1+012*V2+013*V3	47600
B1=D21*V1+D22*V2+D23*V3	47700
C1=D31*V1+D32*V2+D33*V3	47800
IF((AMINI(V1,V2,V3).LT.KTOE).AND.(IDXETA.EQ.4)) GO TO 520	47900
IF((NN.LT.NI).OR.(NP.LT.VI)) GO TO 520	47910
REFINED ESTIMATE OF MAXIMUM POWER POINT	47920
.F(IDXETA.NE.3) GO TO 395	47930
IDXETA=4	47940
CALL CRVFIT(CRNT,VOLT,PTKNT,IDXETA,CMAXPOW,PMAXPOW)	47950
CMAXPOW=PMAXPOW/CMAXPOW	47960
TEST FOR ETAMAX	47970
.F(IDXETA.EQ.2) GO TO 396	48000
IF ((ETA.GT.ETA1).OR.(IDXETA.NE.1)) GO TO 397	48010
IDXETA=IDXETA+1	48020
CALL CRVFIT(CRNT,VOLT,PTKNT,IDXETA,CURDNET,PMAXPOW)	48030
DEFMIN=AMINI(ABS(C1-CURDNET),ABS(C2-CURDNET))	48040
RATIO=D11MIN/CURDNET	48050
IF(RATIO.LT.0.003) GO TO 394	48060
IF(IITVAR.EQ.1) GO TO 410	48070
WRITE(6,590)	48080
GO TO 410	48090
COMPUTATION OF CURDNET	48100
CURDNET=AMAX1(C1,C2,C3)+C1*CRFG	48110
NNM3=IN-3	48120
DO 399 NY=2,JNM1,JNM3	48130
I=NS(2,NY)+NS(1,NY)	48140
N2=NS1(2,NY)+NS1(1,NY)	48150
N3=NS2(2,NY)+NS2(1,NY)	48160

Reproduced from
best available copy.

F11=-1.0/(N3-N1)*(N1-N2) 4952
F12=-1.0/(N1-N2)*(N2-N3) 4974
F13=-1.0/(N2-N3)*(N3-N1) 4974
F21=-(N2+N3)*F11 4994
F22=-(N3+N1)*F12 4984
F23=-(N1+N2)*F13 4994
F31=N2*N3*F11 4993
F32=N3*N1*F12 5004
F33=N1*N2*F13 5003
A=F11*C1+F12*C2+F13*C3 5014
B=F21*C1+F22*C2+F23*C3 5019
C=F31*C1+F32*C2+F33*C3 5024
NSRF=A MIN1(N1, N2, N3)*RF 5029
CURDTRY=A*NSRF+NSRF+B*VSRF+C 5034
399 CURDNET=A MIN1(CJRDNET, CURDTRY) 5037
C
C INTERPOLATION FOR NS
C
410 CURDNTS=CJRDNET*CURDNET 5040
DO 420 NX=1, IN 5050
DO 420 NY=1, JN 5060
NS3(NX, NY)=NS2(NX, NY) 5075
NS2(NX, NY)=NS1(NX, NY) 5080
NS1(NX, NY)=NS(NX, NY) 5090
A=D11*NS1(NX, NY)+D12*NS2(NX, NY)+D13*NS3(NX, NY) 5100
B=D21*NS1(NX, NY)+D22*NS2(NX, NY)+D23*NS3(NX, NY) 5110
C=D31*NS1(NX, NY)+D32*NS2(NX, NY)+D33*NS3(NX, NY) 5120
420 NS(NX, NY)=A*CJRDNTS+B*CURDNET+C 5130
C
C INTERPOLATION FOR MAGI
C
DO 430 NX=2, IHM1 5140
DO 430 NY=2, JHM1 5150
MAGI3(NX, NY)=MAGI2(NX, NY) 5160
MAGI2(NX, NY)=MAGI1(NX, NY) 5170
MAGI1(NX, NY)=MAGI(NX, NY) 5180
A=D11*MAGI1(NX, NY)+D12*MAGI2(NX, NY)+D13*MAGI3(NX, NY) 5190
B=D21*MAGI1(NX, NY)+D22*MAGI2(NX, NY)+D23*MAGI3(NX, NY) 5200
C=D31*MAGI1(NX, NY)+D32*MAGI2(NX, NY)+D33*MAGI3(NX, NY) 5210
430 MAGI(NX, NY)=A*CJRDNTS+B*CURDNET+C 5220
PTKNT=PTKNT+1 5230
440 ETAL=ETA 5240
GO TO 40 5250
C
C CHECK AND INCREMENT MESHKNT 5260
C
450 MESHKNT=MESHKNT+1 5270
C
C BEGIN REMESHING BY STORING NS IN DUMMY AND MAGI IN DUMAG 5280
C
IX=1 5290
DO 470 NX=1, IN 5300
IY=1 5310
DO 460 NY=1, JN 5320
DUMMY(IX, IY)=NS(NX, NY) 5330
DUMAG(IX, IY)=MAGI(NX, NY) 5340
460 IY=IY+3 5350
470 IX=IX+3 5360
C
C COMPUTE DUMMY AND DUMAG AT HORIZONTAL INTERMEDIATE POINTS 5370
C



```

1. MAX=3*INM1+1
1 LEFT MX=3*JN-5
DO 480 IX=1,IXMAX,3
DO 480 ILEFT=1,ILEFTMX,3
IRIGHT=ILEFT+3
DUMMY(IX,ILEFT+1)=(DJMMY(IX,ILEFT)+DUMMY(IX,ILEFT)+DUMMY(IX,IRIGHT)
EY)/3.0
DUMAG(IX,ILEFT+1)=(DUMAG(IX,ILEFT)+DUMAG(IX,ILEFT)+DUMAG(IX,IRIGHT)
IY)/3.0
DUMMY(IX,ILEFT+2)=(DJMMY(IX,ILEFT)+DUMMY(IX,IRIGHT)+DUMMY(IX,IRIGH
'T))/3.0
480 DUMAG(IX,ILEFT+2)=(DUMAG(IX,ILEFT)+DUMAG(IX,IRIGHT)+DUMAG(IX,IRIGH
'T))/3.0

COMPUTE DJMMY AND DUMAG AT VERTICAL INTERMEDIATE POINTS

ILOWMAX=3*IN-5
IYMAX=3*JNM1+1
DO 490 ILow=1,ILOWMAX,3
DO 490 IY=1,IYMAX
IH,GH=ILow+3
DUMMY(ILow+1,IY)=(DJMMY(ILow,IY)+DUMMY(ILow,IY)+DUMMY(IHIGH,IY))/3
1.0
DUMMY(ILow+2,IY)=(DUMMY(ILow,IY)+DUMMY(IHIGH,IY)+DUMMY(IHIGH,IY))/
13.0
DUMAG(ILow+1,IY)=(DUMAG(ILow,IY)+DUMAG(ILow,IY)+DUMAG(IHIGH,IY))/3
1.0
490 DUMAG(ILow+2,IY)=(DUMAG(ILow,IY)+DUMAG(IHIGH,IY)+DUMAG(IHIGH,IY))/
13.0

TRANSFER DUMMY INTO NEW VS MESH

IN=3*IN-4
JN=3*JN-4
DO 500 NX=1,IN
DO 500 NY=1,JN
IS(NX,NY)=DJMMY(NX+1,NY+1)

TRANSFER DUMAG INTO NEW MAGI MESH
IH=3*IH-4
DO 510 NX=1,IH
DO 510 NY=1,JY
MAUI(NX,NY)=DUMAG(NX+2,NY)

RESET I AND J TO THE NUMBER OF INCREMENTS IN THE NEW MESH
I=I+I+I
J=J+J+J

BEGIN NEW MESH
GO TO 30

SUMMARY WRITEOUT OF VOLTAGE, CURRENT AND EFFICIENCY
N=NI=PIKN1-1
IR+TE (6,500)
DO 520 INDX=1,PIKN1
VOLITMP=VOLT(INDX)
COPITMP=CRAT(INDX)

```

```

ETA=CURDTMP*VOLTTMP/POWMAX
IF(LCJRV.EQ.1) GO TO 530
WRITE(6,610) INDX,CURDTMP,VOLTTMP,ETA
CONTINUE

SUMMARY OF OUTPUT RESULTS
VOC = VOLT(1)
VF=VOC/VGAP
CURDSC=(-BV-SQRT(BV*BV-4.0*AV*CV))/2.0/AV
ETACOL=CJRDS C/CJRDMAX
CF=PMAXPON/VOC/CJRDS C
ETACELL=PMAX PON/POWMAX
WRITE(6,620) VOC, VF, CURDSC, ETACOL, PMAXPON, CMAXPON, VMAXPON, CF,
ETACELL, X0, LN, LP, LI, ENR
FORMAT(/,1X,5HVOC = ,F6.4,/,1X,5HVF = ,F6.4,/,1X,9HCURDSC = ,
E10.3,/,1X,9HETACOL = ,F6.4,/,1X,10HMAXPON = ,E10.3,/,
1X,10HCMAXPON = ,F10.3,/,1X,10HVMAXPON = ,F6.4,/,1X,5HCF = ,
F5.4,/,1X,10HETACELL = ,F6.4,/,1X,5HX0 = ,E10.3,/,1X,5HLN = ,E10.3
3,/,1X,5HLP = ,E10.3,/,1X,5HLI = ,E10.3,/,1X,6HENR = ,E10.3)

STORE OUTPUTS IN VECTORS
VOCD(ID)=VOC
VFD(ID)=VF
CURDSCD(ID)=CJRDS C
CURDMXD(ID)=CJRDMAX
ETACOLD(ID)=ETACOL
PMXPOND(ID)=PMAXPON
CMXPOND(ID)=CMAXPON
VMXPOND(ID)=VMAXPON
CFID(ID)=CF
ETACD(ID)=ETACELL
LNEN(ID)=LN
JNLP(ID)=NLP
X0(IID)=N0
IF(L3PTS.EQ.1) GO TO 730

SELECT NEW MESH PARAMETERS
IF(LC.EQ.1) NLN1=NLNT+1
IF(LC.EQ.2) NLN1=NLNT+1
IF(LC.EQ.3) NLP1=NPT+1
IF(LC.EQ.4) NPT1=NPT+1
IF(LC.EQ.5) NX01=NXOT+1
IF(LC.EQ.6) NX01=NXOT+1

HAVE OUTPUTS BEEN EVALUATED FOR NEW MESH PARAMETERS
IEL=IEVAL(NL1, NLP1, NX01)
IF(IE1.EQ.0) GO TO 5

IS POWER OUTPUT FOR NEWEST MESH GREATER THAN MAXIMUM POWER
OUTPUT FROM PREVIOUS MESHES
IF(IE1.EQ.1) GO TO 5
IF(VOLTTMP.GT.VOLTTMP1) GO TO 720
VOLTTMP1=VOLTTMP
IE1=IE1+1
GO TO 5
IE1=IE1-1
NLP1=NLP1+1

```

NXOT=NX01
IDXXOM=3
IT=IC
I3PTS=0
GO TO 700

HAS THE POWER OUTPUT BEEN EVALUATED FOR THE SIX MESH ARRANGEMENTS ADJASCENT TO THE MESH MAXIMUM POWER POINT

720 IC=IC+1
IF(IC.EQ.7) IC=1
NLNT=NLNT
NLPT=NLPT
NXOT=NXOT
IF(IC.NE.IT) GO TO 700

EVALUATION OF OUTPUT PARAMETERS FOR 3 ADDITIONAL POINTS

I3PTS=1
JLNP=IEVAL(NLNT+1,NLPT,NXOT)
JLNM=IEVAL(NLNT-1,NLPT,NXOT)
JLPP=IEVAL(NLNT,NLPT+1,NXOT)
JLPM=IEVAL(NLNT,NLPT-1,NXOT)
JXOP=IEVAL(NLNT,NLPT,NXOT+1)
JXOM=IEVAL(NLNT,NLPT,NXOT-1)
ICLN=-1
IF(PMXPCWD(JLNP).GT.PMXPOWD(JLNM)) ICLN=1
RICLN=ICLN
ICLP=-1
IF(PMXPCWD(JLPP).GT.PMXPOWD(JLPM)) ICLP=1
RCLP=ICLP
ICXD=-1
IF(PMXPOWD(JXOP).GT.PMXPOWD(JXOM)) ICXD=1
RCXO=ICXD

730 LNLP=IEVAL(NLNT+ICLN,NLPT+ICLP,NXOT)
LNXO=IEVAL(NLNT+ICLN,NLPT,NXOT+ICXO)
LPXO=IEVAL(NLNT,NLPT+ICLP,NXOT+ICXO)
NLNT=NLNT+ICLN
NLPT=NLPT+ICLP
NXOT=NXOT
IF(INLP.EQ.0) GO TO 5
IF(PMXPOWD(IET).LT.PMXPOWD(LNLP)) GO TO 710
NLPT=NLPT
NXOT=NXOT+ICXO
IF(NXOT.EQ.NXOMIN) GO TO 732
IF(LNXO.EQ.0) GO TO 5
IF(PMXPCWD(IET).LT.PMXPOWD(LNXO)) GO TO 710
NLNT=NLNT
NLPT=NLPT+ICLP
IF(LPXO.EQ.0) GO TO 5
IF(PMXPOWD(IET).LT.PMXPOWD(LPXO)) GO TO 710

EVALUATION OF COEFFICIENTS FOR POWER IN SECOND ORDER EXPANSION

740 CALL COFFF(PMXPOWD)

USE OF LIBRARY SUBROUTINE TO FIND INTERPOLATED MAXIMUM POWER POINT

750 CALL NMFGOLAR(BM,XM,3, IDXXW,1, ISZ)
IF(CSEVNE.0) GO TO 750

*Reproduced from
best available copy.*

IF(IDXXDM.EQ.2) XM(3,1)=0
 D 735 NX=1,3
 XM(NX,1)=-0.5*XM(NX,1)

EVALUATION OF OJPUTS AT INTERPOLATED MAXIMUM POWER POINT

PMAXPOW=D(PMXPOWD(IET),BM,AM,XM)

NLN=NLNT

NLP=NLP

NXO=NXT

NLN=NLN+XM(1,1)

NLP=NLP+XM(2,1)

NXO=NXO+XM(3,1)

WRIT(E(6,660) NLN,NLP,NXO,AM,BM

FORMAT(3E13.3)

IF(AM(1,2).EQ.0.0) GO TO 737

CALL EIGEN(AM,EIGVAL,3,IDXDM,1)

WRIT(E(6,560)

WRIT(E(6,660) EIGVAL,AM

CALL COEFF(CMXPOWD)

CMAXPOW=D(CMXPOWD(IET),BM,AM,XM)

CALL COEFF(VOC0D)

VOC=D(VOC0D(IET),BM,AM,XM)

CALL COEFF(CJRDS0D)

CURDSC=D(CJRDS0D(IET),BM,AM,XM)

CALL COEFF(CJRDMXD)

IRDMAX=D(CJRDMXD(IET),BM,AM,XM)

VOC=VOC/VGAP

CJRC0L=CJRDS/C/CJRDMAX

MAXPOW=PMAXPOW/CMAXPOW

=CMAXPOW/VOC/CJRDS

FELL=VF*CF*ETAC0L

VK=VGAP*CIRDMAX

VF=CF*VK/2.0

CF=PVK*2.0

C=NX0*RI

. AND WRITEOPTS

WRIT(E(6,625) H,C,L,I,CURDOPT,ISP

DRHAI(7,7,1X,4H0) ,E9.3,2X,4H0 = ,E9.3,2X,5H1I = ,E9.3,2X,

10CURD0PT = ,E9.3,2X,6H1SE = ,I1,/,/)

TE(6,630)

FORMAT(1X,3H0D,3H0N,3H0P,3H0J,6HVJC,6HVF,10HCURDSC,

10AG,10HCIRDMAX,10HCMAXPOW,6HVMAXPW,10IPMAXPOW,

10CF,6.3E1AC0L,/)

TE(740 IP-1,10

WRIT(E(6,640) IP,JNL4(IP),JNL2(IP),JNL1(IP),V0D(IP),VFD(IP),

CFPS0D(IP),ETAC0L(IP),CIRDMXD(IP),CMXPOWD(IP),VMXPOWD(IP),

PRXP0W(IP),CFD(IP),ETAD(IP))

TE(740 41B,2E6.4,F10.3,F6.4,2E10.3,F6.4,E10.3,2E6.4)

V0D(IP),VFD(IP),V0C(IP),VJC,VI,CURDSC,ETAC0L,CURDMAX,CMAXPOW,

CMXPOW,PRXP0W,PRDMAX,CF,ETAFELL

TE(740 7,7,8H0N,-E10.3,7,5H0LF,-E10.3,7,5H0X0,-E10.3,7,

5H0S,-E10.3,7,5H0V0C,-E10.3,7,5H0V0D,-E10.3,7,5H0ETAC0L = ,

5H0V0C,-E10.3,7,5H0V0D,-E10.3,7,5H0ETAC0L = ,5H0V0C,-E10.3,7,5H0V0D,-E10.3,7,5H0ETAC0L = ,

5H0V0C,-E10.3,7,5H0V0D,-E10.3,7,5H0ETAC0L = ,5H0V0C,-E10.3,7,5H0V0D,-E10.3,7,5H0ETAC0L = ,

5H0V0C,-E10.3,7,5H0V0D,-E10.3,7,5H0ETAC0L = ,

AM(1,1)=AM(2,1)=0	78530
AM(3,1)=AM(1,3)=0	78540
AM(2,3)=AM(3,2)=0	78550
GO TO 733	78550
	78700
FORMAT (1X,17HS JCESS FJLL EXIT ,/)	78800
FORMAT (1X,5(2X,E13.6))	78900
FORMAT (1X)	79000
FORMAT (1X,9HMESHKNT =,I4,9HLDOPKNT =,I4,/)	79100
FORMAT (/,,/,,1X,9HMESHKNT =,I2,1X,9HPATHKNT =,I2,/)	79200
FORMAT (/,,/,,1X,27H MAXIMUM EFFICIENCY VALUES ,/,/)	79300
FORMAT (/,,/,,1X,5HPTKNT,6X,7HCURDNET,8X,7HVOLTAGE,8X,3HETA,/)	79400
FORMAT (1X,15,4(5X,E10.3))	79500
FORMAT(12X,E12.4)	79550
END	79600

SUBROUTINE COEFF(DM)
COMMON IET,JLN_P,JLN_M,JLPP,JLP_M,JXDP,JXM_M,LN_P,LN_{X0},LPX₀,RICLN,
+ LCLP,RICKC,BM(3,1),AM(3,3),JLN_N(50),JLN_P(50),JX_N(50),ID
DIMENSION DM(50) 79700
AM(1,1)=(DM(JLN_P)+DM(JLN_N))/2.0-DM(IET) 79800
BM(1,1)=(DM(JLN_P)-DM(JLN_N))/2.0 79900
AM(2,2)=(DM(JLPP)+DM(JLP_M))/2.0-DM(IET) 80000
BM(2,1)=(DM(JLPP)-DM(JLP_M))/2.0 80100
AM(3,3)=(DM(JXDP)+DM(JXDM))/2.0-DM(IET) 80200
BM(3,1)=(DM(JXDP)-DM(JXDM))/2.0 80300
AM(1,2)=AM(2,1)=(DM(LN_P)-DM(IET)-BM(1,1)*RICLN-BM(2,1)*RCLP 80400
+ -AM(1,1)-AM(2,2))/2.0/RICLN/RCLP 80500
AM(1,3)=AM(3,1)=0. 80600
AM(2,3)=AM(3,2)=0. 80700
IF ((LN_{X0}.EQ.0).OR.(LPX₀.EQ.0)) RETURN 80800
AM(1,3)=AM(3,1)=(DM(LN_{X0})-DM(IET)-BM(1,1)*RICLN-BM(3,1)*RICXO 80900
+ -AM(1,1)-AM(3,3))/2.0/RICLN/RICXO 81000
AM(2,3)=AM(3,2)=(DM(LPX₀)-DM(IET)-BM(2,1)*RCLP-BM(3,1)*RICXO 81100
+ -AM(2,1)-AM(3,3))/2.0/RCLP/RICXO 81200
RETURN 81300
END 81400

```
FUNCTION C(DIET,BM,AM,XM)
DIMENSION AM(3,3),BM(3,1),XM(3,1)
D=DIET
DO 800 I=1,3
D=D+BM(I,1)*XM(I,1)
DO 800 J=1,3
D=D+AM(I,J)*XM(I,1)*XM(J,1)
RETURN
END
```

815.00
81 30
817.00
818.00
819.00
820.00
821.00
822.00
823.00

FUNCTION IEVAL(NLN1,NLP1,NX01)	824
COMMON IET,JLNP,JLNM,JLPP,JLPM,JXJP,JXOM,LNLP,LNXO,LPXO,RICLN,	825
IRICLP,RICXC,BM(3,1),AM(3,3),JNLN(50),JNLP(50),JNXO(50),ID	825
IP=0	827
IEVAL=0	828
810 IF(IP.EQ.ID) RETURN	829
IP=IP+1	830
IF(NLN1.NE.JNLN(IP)) GO TO 810	831
IF(NLP1.NE.JNLP(IP)) GO TO 810	832
IF(NX01.NE.JNXO(IP)) GO TO 810	833
IEVAL=IP	834
RETURN	835
END	836

ROUTINE CRVFIT(CRNT, VOLT, PTKNT, INDEXTA, CURONET, PMAXPOW)	83700
CALL CRVFIT(CRNT, VOLT, PTKNT, INDEXTA, CURONET, PMAXPOW)	83800
DEFINITION VOLT(30), CRNT(30), CM(30,30), T(30), TIM1(30), POWER(30)	83900
A(30)	84000
END	84100
END	84200
END	84300
END	84400
END	84500
END	84600
END	84700
END	84800
K1=AMAX1(CRNT(PTKNT), CRNT(PTKNT-1), CRNT(PTKNT-2))	84900
K2=AMAX1(POWER(PTKNT), POWER(PTKNT-1))	85000
L1=1, PTKNT	85100
M1, L1=1	85200
CRNT(I)=CRNT(I)-SKEN*POWER(I)	85300
DO J=2, PTKNT	85400
M(I,J)=CM(I,J-1)*CRNT(J)	85500
CALL LINEQ1(CM, POWER, T, 30, PTKNT, 1, ILE)	85600
IF(IFF(6,3) .NE.	85700
FORMAT(SHIFT = ,11)	85800
SEND THE MAXIMUM POWER POINT	85900
DO I=2, PTKNT	86000
IM1=I-1	86100
IM2=I+1	86200
P1=CRNT(PTKNT)	86300
P2=CRNT(PTKNT-1)	86400
P3=CRNT(PTKNT+1)	86500
PP1=P1*(P1-IM1)*(P1-CRNT1)	86600
PP2=P2*(P2-IM1)*(P2-CRNT2)	86700
PP3=P3*(P3-IM2)*(P3-CRNT3)	86800
PP12=(PP1+PP2+PP3)/3	86900
PP12=PP12*(PP12-PP1)*(PP12-PP2)	87000
P12=PP12/PP12	87100
P12=CRNT1	87200
IM1=CURONET	87300
INDEXTA	87400
COMPUTATION OF MAXIMUM POWER	87500
PMAXPOW=0.	87600
IM1=1	87700
DO I=2, PTKNT	87800
PMAXPOW=PMAXPOW+(T(I)*CRNT(I))	87900
INDEXTA=INDEXTA+1	88000
P12=CURONET	88100
INDEXTA=INDEXTA+1	88200
PMAXPOW=PMAXPOW+(T(I)*CRNT(I))	88300
INDEXTA=INDEXTA+1	88400
P12=CURONET	88500
INDEXTA=INDEXTA+1	88600
PMAXPOW=PMAXPOW+(T(I)*CRNT(I))	88700
INDEXTA=INDEXTA+1	88800
P12=CURONET	88900
INDEXTA=INDEXTA+1	89000

Reproduced from
best available copy.

WAVE E X=ALIPLANT, Y=0, Z=0	8870
WAVE PTKNT	8900
WAVE TIM1(30)	8910
WAVE	8920
WAVE=0	8930
WAVE, PTKNT	8940
WAVE=PERIM+TIME(1)*CTM2	8950
WAVE=GEN2*CORDNET	8960
WAVE	8970
WAVE	8980

	1.0644E1	
	0.3113E19	
	3.4637E14	
1.100F-03	3.7778E+19	2.6068E+21
1.100L-03	4.0325E+19	1.6745E+21
1.100F-03	4.2154E+19	1.2834E+21
1.100E-03	4.3532E+19	1.0335E+21
1.150E-13	4.4772E+19	8.6096E+20
1.20E-03	4.5764E+19	7.3683E+20
1.200E-03	4.6625E+19	6.4419E+20
1.200F-02	4.7384E+19	5.7268E+20
1.1250E-02	4.8253E+19	5.1579E+20
1.250E-02	4.8578E+19	4.6935E+20
1.1750E-02	4.9233E+19	4.3059E+20
1.2000E-02	4.9756E+19	3.9764E+20
1.5250E-02	5.0235E+19	3.6921E+20
1.7500E-02	5.0681E+19	3.4439E+20
1.8750E-02	5.1047E+19	3.2247E+20
2.0000E-02	5.1488E+19	3.0296E+20
2.1250E-02	5.1856E+19	2.8547E+20
2.2500E-02	5.2202E+19	2.6970E+20
2.3750E-02	5.2531E+19	2.5540E+20
2.5000E-02	5.2842E+19	2.4237E+20
2.6250E-02	5.3137E+19	2.3046E+20
2.7500E-02	5.3418E+19	2.1952E+20
2.8750E-02	5.3686E+19	2.0945E+20
3.0000E-02	5.3942E+19	2.0016E+20
3.1250E-02	5.4187E+19	1.9155E+20
3.2500E-02	5.4421E+19	1.8356E+20
3.3750E-02	5.4646E+19	1.7617E+20
3.5000E-02	5.4862E+19	1.6919E+20
3.6250E-02	5.5075E+19	1.6272E+20
3.7500E-02	5.5269E+19	1.5666E+20
3.8750E-02	5.5451E+19	1.5097E+20
4.0000E-02	5.5646E+19	1.4564E+20
4.1250E-02	5.5825E+19	1.4061E+20
4.2500E-02	5.5978E+19	1.3588E+20
4.3750E-02	5.6165E+19	1.3142E+20
4.5000E-02	5.6327E+19	1.2720E+20
4.6250E-02	5.6483E+19	1.2321E+20
4.7500E-02	5.6615E+19	1.1943E+20
4.8750E-02	5.6742E+19	1.1585E+20
5.0000E-02	5.6823E+19	1.1244E+20
5.1250E-02	5.6924E+19	1.0921E+20
5.2500E-02	5.7117E+19	1.0613E+20
5.3750E-02	5.7328E+19	1.0320E+20
5.5000E-02	5.7455E+19	1.0042E+20
5.6250E-02	5.7579E+19	9.7730E+19
5.7500E-02	5.7711E+19	9.5182E+19
5.8750E-02	5.7817E+19	9.2749E+19
6.0000E-02	5.7932E+19	9.0413E+19
6.1250E-02	5.8043E+19	8.8183E+19
6.2500E-02	5.8152E+19	8.6047E+19
6.3750E-02	5.8251E+19	8.3988E+19
6.5000E-02	5.8342E+19	8.1924E+19
6.6250E-02	5.8434E+19	7.9850E+19
6.7500E-02	5.8523E+19	7.7870E+19
6.8750E-02	5.8615E+19	7.5890E+19
7.0000E-02	5.8704E+19	7.4874E+19

7.2500E-02	5.8937E+19	7.1693E+19
7.3750E-02	5.9026E+19	7.0188E+19
7.5000E-02	5.9113E+19	6.8735E+19
7.6250E-02	5.9198E+19	6.7334E+19
7.7500E-02	5.9281E+19	6.5980E+19
7.8750E-02	5.9363E+19	6.4673E+19
8.0000E-02	5.9443E+19	6.3408E+19
8.1250E-02	5.9521E+19	6.2186E+19
8.2500E-02	5.9598E+19	6.1003E+19
8.3750E-02	5.9674E+19	5.9858E+19
8.5000E-02	5.9748E+19	5.8749E+19
8.6250E-02	5.9821E+19	5.7675E+19
8.7500E-02	5.9892E+19	5.6633E+19
8.8750E-02	5.9962E+19	5.5623E+19
9.0000E-02	6.0031E+19	5.4644E+19
9.1250E-02	6.0099E+19	5.3693E+19
9.2500E-02	6.0165E+19	5.2770E+19
9.3750E-02	6.0231E+19	5.1874E+19
9.5000E-02	6.0295E+19	5.1004E+19
9.6250E-02	6.0358E+19	5.0157E+19
9.7500E-02	6.0420E+19	4.9335E+19
9.8750E-02	6.0482E+19	4.8535E+19
1.0000E-01	6.0542E+19	4.7757E+19